Chapter 8: Inviscid Incompressible Flow: a Useful Fantasy

8.1 Introduction

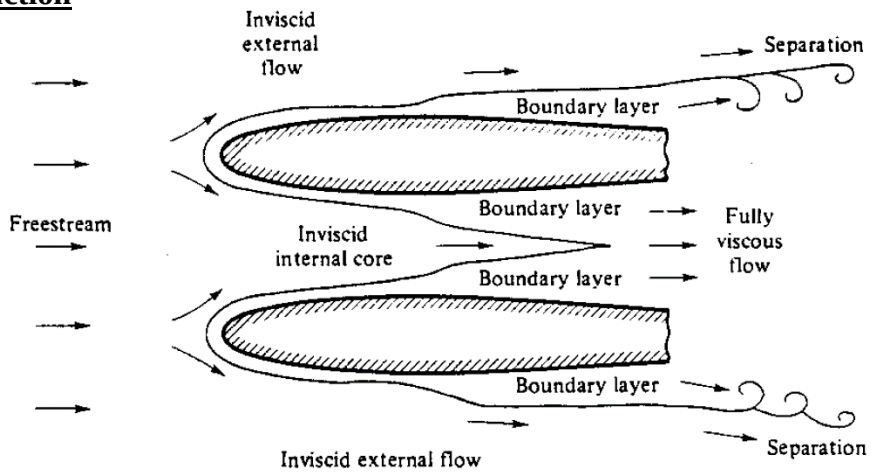

For high Re external flow about streamlined bodies viscous effects are confined to boundary layer and wake region. For regions where the BL is thin i.e. favorable or weak adverse pressure gradient regions, Viscous/Inviscid interaction is weak and traditional BL theory can be used. For regions where BL is thick and/or the flow is separated i.e. strong adverse pressure gradient regions more advanced boundary layer theory must be used including Viscous/Inviscid interactions.

For internal flows at high Re viscous effects are always important except near the entrance. Recall that vorticity is generated in regions with large shear. Therefore, outside the B.L and wake and if there is no upstream vorticity then $\underline{\omega}=0$ is a good approximation.
Note that for compressible flow this is not the case in regions of large entropy gradient. Also, we are neglecting non-inertial effects and other mechanisms of vorticity generation.

Potential flow theory

1) Determine ϕ from solution to Laplace equation

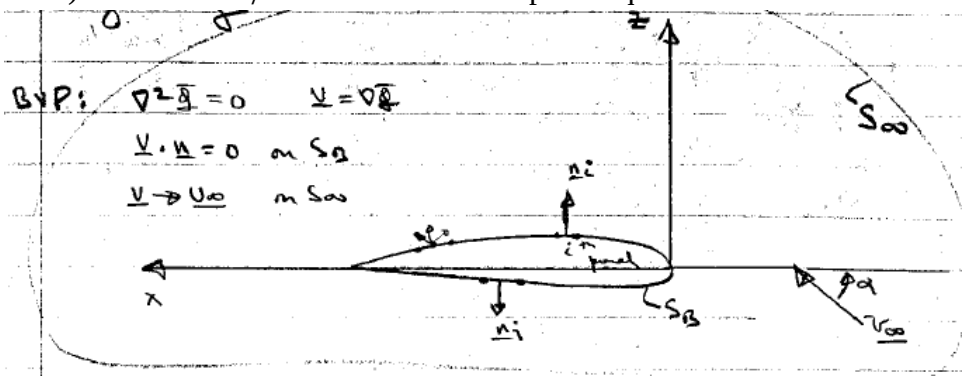

$$\frac{DF}{Dt} = 0 \to \frac{\partial F}{\partial t} + \underline{V}.\nabla F = 0 \to \underline{V}.\underline{n} = -\frac{1}{|\nabla F|}\frac{\partial F}{\partial t} \quad \text{for steady flow } \underline{V}.\underline{n} = 0$$

(F=surface function = z-ζ)

2) Determine $\underline{V}$ from $\underline{V}=\nabla\phi$ and p(x) from Bernoulli equation

Therefore, primarily for external flow application we now consider inviscid flow theory ($\mu=0$) and incompressible flow ($\rho=const$)

Euler equation:

$$\nabla.\underline{V}=0$$

$$\rho\frac{D\underline{V}}{Dt}=-\nabla p+\rho\underline{g}$$

$$\rho\frac{\partial V}{\partial t}+\rho\underline{V}.\nabla\underline{V}=-\nabla(p+\gamma z)$$

$$\underline{V}.\nabla\underline{V}=\nabla\frac{V^2}{2}-\underline{V}\times\underline{\omega}$$

$$Where:\ \underline{\omega}=\nabla\times\underline{V}=vorticity=2\times\ fluid\ angular\ velocity$$

$$\Rightarrow\rho\frac{\partial\underline{V}}{\partial t}+\nabla(p+\frac{1}{2}\rho V^2+\gamma z)=\rho\underline{V}\times\underline{\omega}$$

If $\underline{\omega}=0$ *ie* $\nabla\times\underline{V}=0$ *then* $\underline{V}=\nabla\phi$:

$$\boxed{\rho\frac{\partial\phi}{\partial t}+p+\frac{1}{2}\rho\nabla\phi\cdot\nabla\phi+\gamma z=B(t)}$$

Continuity equation shows that GDE for ϕ is the Laplace equation which is a 2nd order linear PDE ie superposition principle is valid. (Linear combination of solution is also a solution)

$$\nabla\cdot\underline{V}=\nabla\cdot\nabla\phi=\nabla^2\phi=0$$

$$\phi=\phi_1+\phi_2$$

$$\nabla^2\phi=0\Rightarrow\nabla^2(\phi_1+\phi_2)=0\Rightarrow\nabla^2\phi_1+\nabla^2\phi_2=0\Rightarrow\begin{cases}\nabla^2\phi_1=0\\ \nabla^2\phi_2=0\end{cases}$$

Techniques for solving Laplace equation:

1) superposition of elementary solution (simple geometries)
2) surface singularity method (integral equation)
3) FD or FE
4) electrical or mechanical analogs
5) Conformal mapping (for 2D flow)
6) Analytical for simple geometries (separation of variable etc)

8.2 Elementary plane-flow solutions:

Recall that for 2D we can define a stream function such that:

$u = \psi_y$

$v = -\psi_x$

$$\omega_z = v_x - u_y = \frac{\partial}{\partial x}(-\psi_x) - \frac{\partial}{\partial y}(\psi_y) = -\nabla^2\psi = 0$$

i.e. $\nabla^2\psi = 0$

Also recall that ϕ and ψ are orthogonal.

$u = \psi_y = \phi_x$

$v = -\psi_x = \phi_y$

$d\phi = \phi_x dx + \phi_y dy = udx + vdy$

$d\psi = \psi_x dx + \psi_y dy = -vdx + udy$

i.e. $$\left.\frac{dy}{dx}\right|_{\phi=const} = -\frac{u}{v} = \frac{-1}{\left.\frac{dy}{dx}\right|_{\psi=const}}$$

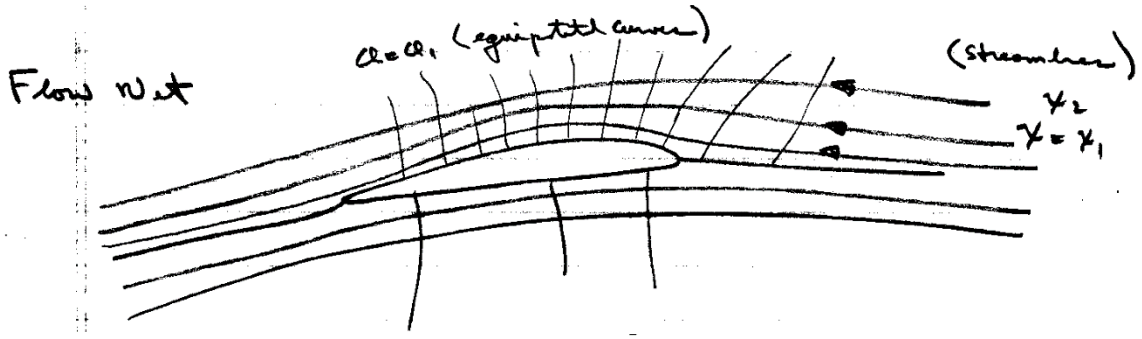

Uniform stream

$u = U_\infty = \psi_y = \phi_x = const$

$v = 0 = -\psi_x = \phi_y$

i.e. $\phi = U_\infty x$

$\psi = U_\infty y$

Note: $\nabla^2\phi = \nabla^2\psi = 0$ is satisfied.

$\underline{V} = \nabla\phi = U_\infty \hat{i}$

Say a uniform stream is at an angle α to the x-axis:

$$u = U_\infty \cos\alpha = \frac{\partial\psi}{\partial y} = \frac{\partial\phi}{\partial x}$$

$$v = U_\infty \sin\alpha = -\frac{\partial\psi}{\partial x} = \frac{\partial\phi}{\partial y}$$

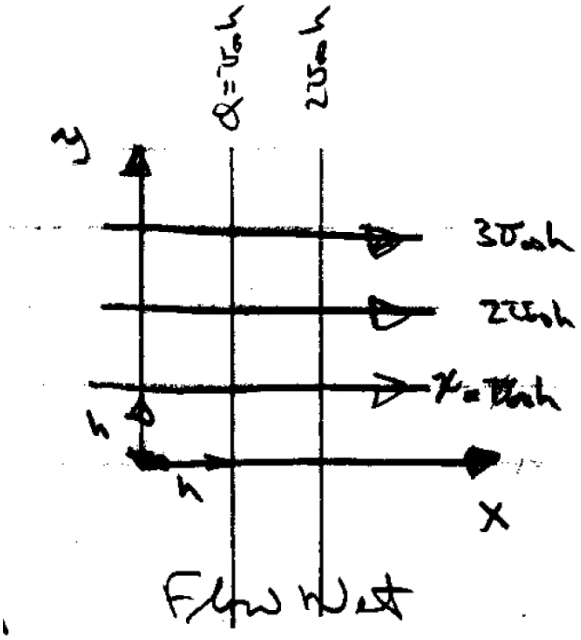

After integration, we obtain the following expressions for the stream function and velocity potential:

$$\psi = U_\infty \left(y\cos\alpha - x\sin\alpha \right)$$
$$\phi = U_\infty \left(x\cos\alpha + y\sin\alpha \right)$$

2D Source or Sink:

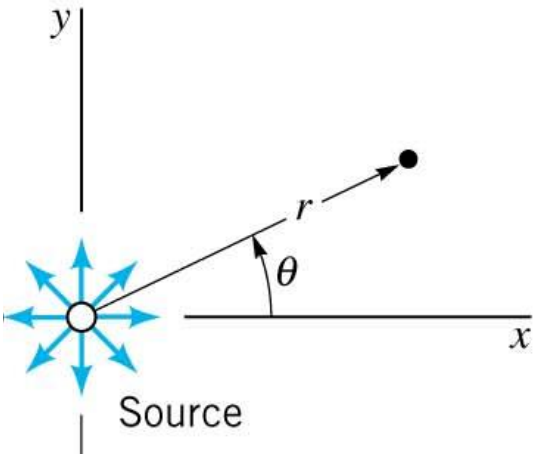

$$x = r\cos\theta$$
$$y = r\sin\theta$$

Imagine that fluid comes out radially at origin with uniform rate in all directions. (singularity at origin where velocity is infinite)

Consider a circle of radius r enclosing this source. Let v_r be the radial component of velocity associated with this source (or sink). Then, from conservation of mass, for a cylinder of radius r, and width b, perpendicular to the paper,

$$Q = \int_A \underline{V} \cdot d\underline{A} \quad \left[\frac{L^3}{S} \right] \text{ where } \underline{V} = v_r \hat{e_r};\ \underline{n} = \hat{e_r};\ dA = rd\theta b$$

$$Q = \left(2\pi r\right)\cdot\left(b\right)\cdot v_r$$

$$Or,$$

$$v_r = \frac{Q}{2\pi br}$$

$$\Rightarrow v_r = \frac{m}{r},\ v_\theta = 0$$

Where: $m = \dfrac{Q}{2\pi b}$ is the source strength with unit m^2/s velocity × length

(m>0 for source and m<0 for sink). Note that $\underline{V}$ is singular at (0,0) since $v_r \to \infty$

In a polar coordinate system, for 2-D flows we will use:

$$\underline{V} = \nabla\phi = \frac{\partial\phi}{\partial r}\hat{e_r} + \frac{1}{r}\frac{\partial\phi}{\partial\theta}\hat{e_\theta}$$
$$\nabla = \frac{\partial}{\partial r}\hat{e_r} + \frac{1}{r}\frac{\partial}{\partial\theta}\hat{e_\theta}$$

And:

$$\nabla.\underline{V} = 0$$

$$\frac{1}{r}\frac{\partial}{\partial r}(rv_r) + \frac{1}{r}\frac{\partial}{\partial \theta}(v_\theta) = 0$$

i.e.:

$$v_r = \text{Radial velocity} = \frac{\partial \phi}{\partial r} = \frac{1}{r}\frac{\partial \psi}{\partial \theta}$$

$$v_\theta = \text{Tangential velocity} = \frac{1}{\mathrm{r}}\frac{\partial \phi}{\partial \theta} = -\frac{\partial \psi}{\partial r}$$

Such that $\nabla \cdot \underline{V} = 0$ by definition.

Therefore,

$$v_r = \frac{\mathrm{m}}{\mathrm{r}} = \frac{\partial \phi}{\partial r} = \frac{1}{r}\frac{\partial \psi}{\partial \theta}$$

$$v_\theta = 0 = \frac{1}{\mathrm{r}}\frac{\partial \phi}{\partial \theta} = -\frac{\partial \psi}{\partial r}$$

$$\phi = m \ln r = m \ln \sqrt{x^2 + y^2}$$

i.e.

$$\psi = m\theta = m \tan^{-1}\frac{y}{x}$$

Doublets:

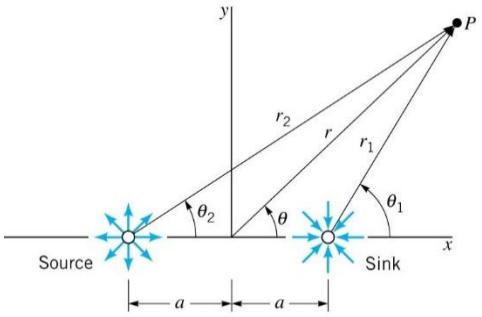

The doublet is defined as:

$$\Psi = -\frac{m}{2\pi}\left(\underbrace{\theta_1}_{sink} - \underbrace{\theta_2}_{source}\right) \rightarrow \theta_1 - \theta_2 = -\frac{2\pi\Psi}{m}$$

$$tan\left(-\frac{2\pi\Psi}{m}\right) = tan(\theta_1 - \theta_2) = \frac{tan\,\theta_1 - tan\,\theta_2}{1 + tan\,\theta_1\, tan\,\theta_2}$$

$$tan\,\theta_1 = \frac{r\,sin\,\theta}{r\,cos\,\theta - a};\;\; tan\,\theta_2 = \frac{r\,sin\,\theta}{r\,cos\,\theta + a}$$

$$tan\left(-\frac{2\pi\Psi}{m}\right) = \frac{2ar\sin\theta}{r^2 - a^2}$$

Therefore

$$\Psi = -\frac{m}{2\pi}\tan^{-1}\left(\frac{2ar\sin\theta}{r^2-a^2}\right)$$

For small distance

$$\Psi = -\frac{m}{\cancel{2}\pi}\frac{\cancel{2}ar\sin\theta}{r^2-a^2} = -\frac{mar\sin\theta}{\pi(r^2-a^2)}$$

The doublet is formed by letting $a \to 0$ while increasing the strength m ($m \to \infty$) so that doublet strength $K = \frac{ma}{\pi}$ remains constant

$$\Psi = -\frac{K\sin\theta}{r}$$

Corresponding potential

$$\phi = \frac{K\cos\theta}{r}$$

By rearranging

$$\Psi = -\frac{K\,\mathrm{rsin}\,\theta}{r^2} = -\frac{Ky}{x^2+y^2} \to x^2 + \left(y+\frac{K}{2\Psi}\right)^2 = \left(\frac{K}{2\Psi}\right)^2 = R^2$$

Plots of lines constant Ψ reveal that streamlines for the doublet are circles through the origin tangent to the x axis as shown in Figure below (equation circle radius R center (h,k) is $(x-h)^2+(y-k)^2=R^2$). Circles show various Ψ = constant above/below x axis

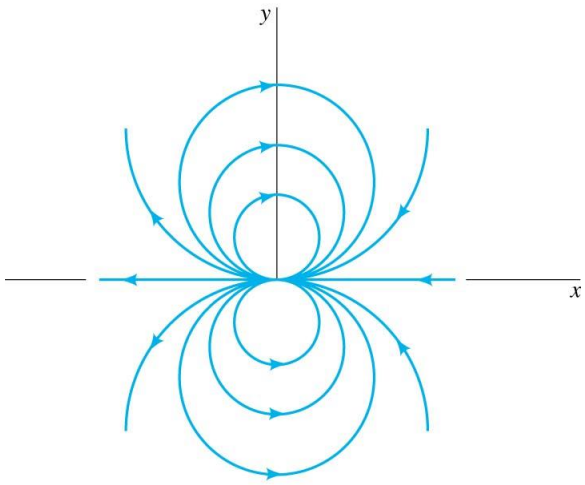

2D vortex:

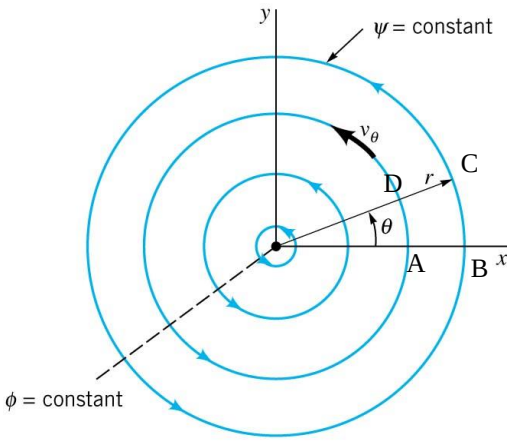

Suppose that value of the ψ and ϕ for the source are reversed.

$v_r = 0$

$$v_\theta = \frac{1}{r}\frac{\partial \phi}{\partial \theta} = -\frac{\partial \psi}{\partial r} = \frac{K}{r}$$

Purely circulatory flow with $v_\theta \to 0$ like 1/r. Integration results in:

$\phi = K\theta$

$\psi = -K \ln r$ **K=constant**

2D vortex is irrotational everywhere except at the origin where $\underline{V}$ and $\underline{V} \times \nabla$ are infinity.

Circulation

Circulation is defined by:

$$\Gamma = \oint_{C=closed\ \ contour} \underline{V} \cdot d\,\underline{s} \qquad \text{For irrotational flow}$$

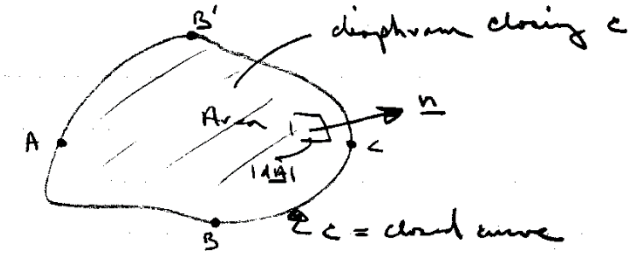

Or by using Stokes theorem: (if no singularity of the flow in A)

$$\Gamma = \oint_{c} \underline{V} \cdot d\,\underline{s} = \iint_{A} \nabla \times \underline{V} \cdot d\,\underline{A} = \iint_{A} \underline{\omega} . \underline{n} dA = \mathbf{0}$$

Therefore, for potential flow $\Gamma = 0$ in general.

However, this is not true for the point vortex due to the singular point at vortex core where $\underline{V}$ and $\underline{V} \times \nabla$ are infinity.

If singularity exists: Free vortex $\upsilon_\theta = \dfrac{K}{r}$

$$\Gamma = \int_0^{2\pi} \underbrace{v_\theta \hat{e}_\theta}_{\underline{V}} \cdot \underbrace{r d\theta \hat{e}_\theta}_{d\underline{s}} = \int_0^{2\pi} \frac{K}{r}(r d\theta) = \underline{2\pi K} \quad \textbf{and} \quad K = \frac{\Gamma}{2\pi}$$

Note: for point vortex, flow still irrotational everywhere except at origin itself where $\underline{V} \to \infty$.

For a path not including (0,0) $\Gamma = 0$

$$\Gamma = \int_A^B v_\theta \widehat{e_\theta} \cdot \widehat{e_r} dr + \int_B^C v_\theta \widehat{e_\theta}\, r d\theta \cdot \widehat{e_\theta} + \int_C^D v_\theta \widehat{e_\theta} \cdot \widehat{e_r} dr + \int_D^A v_\theta \widehat{e_\theta} r d\theta \cdot \widehat{e_\theta}$$
$$= \Delta\theta K - \Delta\theta K = 0$$

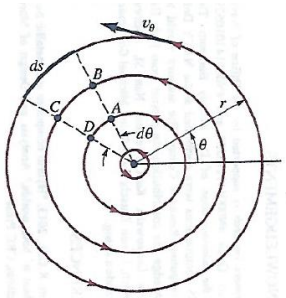

Figure 6.21 Circulation around various paths in a free vortex.

Also, we can use Stokes theorem to show the existence of ϕ:

$$\int_{ABC} \underline{V}\cdot d\underline{s} = \int_{AB'C} \underline{V}\cdot d\underline{s} = \phi_C \quad \text{Since} \quad \int_{ABCB'A} \underline{V}.d\underline{s} = 0$$

Therefore in general for irrotational motion:

$$\int \underline{V}.d\underline{x} = \phi$$

$$\underline{V}\cdot d\underline{x} = d\phi$$

$$\underline{V}\cdot\frac{d\underline{x}}{ds} = \frac{d\phi}{ds} = \nabla\phi.\frac{d\underline{x}}{ds}$$

$$\hat{e}_s = \frac{d\underline{x}}{ds}$$

$$(\underline{V} - \nabla\phi).\hat{e}_s = 0$$

Where: e_s =unit tangent vector along curve x

Since e_s is not zero we have shown:

$$\underline{V} = \nabla\phi$$

i.e. velocity vector is gradient of a scalar function ϕ if the motion is irrotational. ($\oint \underline{V}\cdot d\underline{s} = 0$)

The point vortex singularity is important in aerodynamics, since, distribution of sources and sinks can be used to represent airfoils and wings as we shall discuss shortly. To see this, consider as an example:

an infinite row of vortices:

$$\psi = -K\sum_{i=1}^{\infty} \ln r_i = -\frac{1}{2}K\ln\left[\frac{1}{2}(\cosh\frac{2\pi y}{a} - \cos\frac{2\pi x}{a})\right]$$

Where r_i is radius from origin of ith vortex.

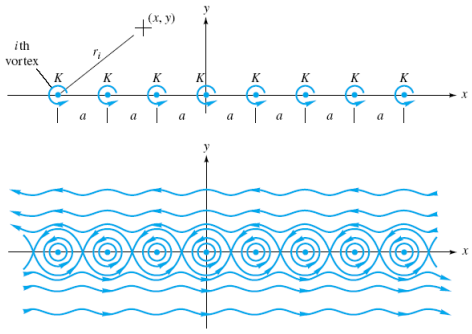

Superposition infinite row equally spaced vortices of equal strength

For $|y| \geq a$ the flow approaches uniform flow with

$$u = \frac{\partial \psi}{\partial y} = \pm \frac{\pi K}{a}$$

+: below x axis
-: above x axis
Note: this flow is just due to infinite row of vortices and there isn't any pure uniform flow

Vortex sheet:
From afar (i.e. $|y| \geq a$) looks like a thin sheet with velocity discontinuity.

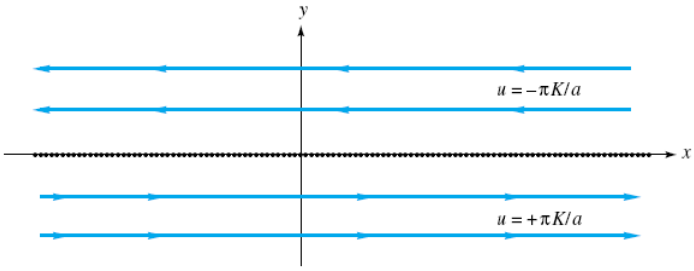

Define $\gamma = \frac{2\pi K}{a}$ = strength of vortex sheet

$d\Gamma = \underline{V} \cdot d\,\underline{s}$ (around closed contour)

$$d\Gamma = u_l dx - u_u dx = (u_l - u_u)dx = \frac{2\pi K}{a} dx$$

i.e. $\gamma = \frac{d\Gamma}{dx}$ =Circulation per unit span

Note: There is no flow normal to the sheet so that vortex sheet can be used to simulate a body surface. This is the basis of airfoil theory where we let $\gamma = \gamma(x)$ to represent body geometry.

Vortex theorem of Helmholtz: (important role in the study of the flow about wings)

1) The circulation around a given vortex line is constant along its length
2) A vortex line cannot end in the fluid. It must form a closed path, end at a boundary or go to infinity.
3) No fluid particle can have rotation, if it did not originally rotate

8.3 Potential Flow Solutions for Simple Geometries

Circular cylinder (without rotation):

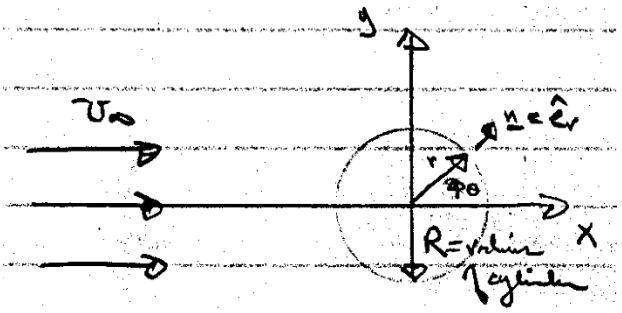

In the previous we derived the following equation for the doublet:

$$\psi_{Doublet=} = -\frac{\lambda y}{x^2+y^2} = -\frac{\lambda \sin\theta}{r}$$

When this doublet is superposed with a uniform flow parallel to the x- axis, we get:

$$\psi = U_\infty r\sin\theta - \frac{\lambda\sin\theta}{r} = U_\infty\left(1-\frac{\lambda}{U_\infty}\frac{1}{r^2}\right)r\sin\theta$$

Where: λ = doublet strength which is determined from the kinematic body boundary condition that the body surface must be a stream surface. Recall that for inviscid flow it is no longer possible to satisfy the no slip condition as a result of the neglect of viscous terms in the GDEs.

The inviscid flow boundary condition is:
F=r-R: Surface Function

$$\frac{DF}{Dt} = 0 \to \frac{\partial F}{\partial t} + \underline{V}.\nabla F = 0 \to \underline{V}\cdot\underline{n} = -\frac{1}{|\nabla F|}\frac{\partial F}{\partial t} = 0 \quad \text{(for steady flow)}$$

Therefore at r=R, $\underline{V}.\underline{n}=0$ i.e. $v_r = 0\big|_{r=R}$.

$$\underline{V} = v_r\hat{e}_r + v_\theta\hat{e}_\theta, \quad \underline{n} = \frac{\nabla F}{|\nabla F|} = \frac{\frac{\partial F}{\partial r}\hat{e}_r + \frac{\partial F}{\partial\theta}\hat{e}_\theta}{\sqrt{F_r^2+F_\theta^2}} = \hat{e}_r$$

$$\underline{V}\cdot\underline{n} = v_r = \frac{1}{r}\frac{\partial\psi}{\partial\theta} = U_\infty\left(1-\frac{\lambda}{U_\infty r^2}\right)\cos\theta = 0$$

$$\Rightarrow \lambda = U_\infty R^2$$

If we replace the constant $\frac{\lambda}{U_\infty}$ by a new constant R^2, the above equation becomes:

$$\psi = U_\infty\left(1-\frac{R^2}{r^2}\right)r\sin\theta$$

This radial velocity is zero on all points on the circle r=R. That is, there can be no velocity normal to the circle r=R. Thus this circle itself is a streamline.

We can also compute the tangential component of velocity for flow over the circular cylinder. From equation,

$$v_\theta = -\frac{\partial \psi}{\partial r} = -U_\infty \left(1 + \frac{R^2}{r^2}\right) \sin\theta$$

On the surface of the cylinder r=R, we get the following expression for the tangential and radial components of velocity:

$$v_\theta = -2U_\infty \sin\theta$$

$$v_r = 0$$

The pressure is obtained from Bernoulli's equation:

$$\frac{p}{\rho} + \frac{1}{2}\left(v_r{}^2 + v_\theta{}^2\right) = \frac{p_\infty}{\rho} + \frac{1}{2}U_\infty^2$$

After some rearrangement we get the following non-dimensional form:

$$C_p(r,\theta) = \frac{p - p_\infty}{\frac{1}{2}\rho U_\infty^2} = 1 - \frac{v_r{}^2 + v_\theta{}^2}{U_\infty^2}$$

At the surface, the only velocity component that is non-zero is the tangential component of velocity. Using $v_\theta = -2U_\infty \sin\theta$, we get at the cylinder surface the following expression for the pressure coefficient:

$$C_p = 1 - 4\sin^2\theta$$

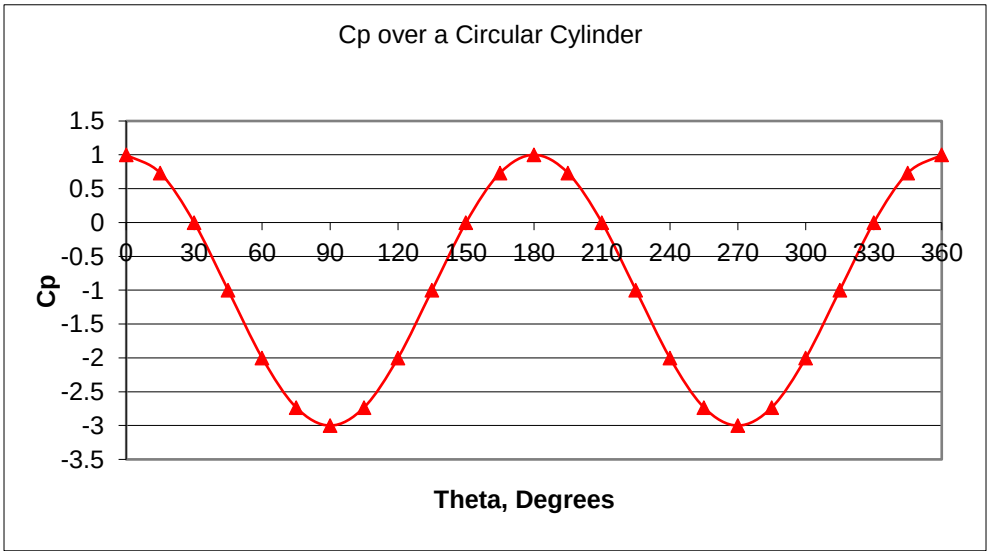

From pressure coefficient we can calculate the fluid force on the cylinder:

$$\underline{F} = -\int_A (p - p_\infty)\underline{n}dA = -\frac{1}{2}\rho U_\infty^2 \int_A C_p(R,\theta)\underline{n}dA$$

$dA = (Rd\theta)b$ b=span length

$$\underline{F} = -\frac{1}{2}\rho U_\infty^2 bR \int_0^{2\pi} (1-4\sin^2\theta)(\cos\theta\,\hat{i} + \sin\theta\,\hat{j})d\theta$$

$$C_L = \frac{Lift}{\frac{1}{2}\rho U_\infty^2 bR} = \frac{\underline{F}\cdot\hat{j}}{\frac{1}{2}\rho U_\infty^2 bR} = -\int_0^{2\pi}(1-4\sin^2\theta)\sin\theta\,d\theta = 0$$ (due to symmetry of flow around x axis)

$$C_D = \frac{Drag}{\frac{1}{2}\rho U_\infty^2 bR} = \frac{\underline{F}\cdot\hat{i}}{\frac{1}{2}\rho U_\infty^2 bR} = -\int_0^{2\pi}(1-4\sin^2\theta)\cos\theta\,d\theta = 0$$ (dÁlembert paradox)

Circular cylinder with circulation:

The stream function associated with the flow over a circular cylinder, with a point vortex of strength Γ placed at the cylinder center is:

$$\psi = U_\infty r\sin\theta - \frac{\lambda\sin\theta}{r} - \frac{\Gamma}{2\pi}\ln r$$

From $\underline{V}.\underline{n}=0$ at r=R: $\lambda = U_\infty R^2$

Therefore, $\psi = U_\infty r\sin\theta - \frac{U_\infty R^2\sin\theta}{r} - \frac{\Gamma}{2\pi}\ln r$

The radial and tangential velocity is given by:

$$v_r = \frac{1}{r}\frac{\partial\psi}{\partial\theta} = U_\infty\left(1-\frac{R^2}{r^2}\right)\cos\theta \qquad v_\theta = -\frac{\partial\psi}{\partial r} = -U_\infty\left(1+\frac{R^2}{r^2}\right)\sin\theta + \frac{\Gamma}{2\pi r}$$

On the surface of the cylinder (r=R):

$$v_r = \frac{1}{r}\frac{\partial\psi}{\partial\theta} = U_\infty\left(1-\frac{R^2}{R^2}\right)\cos\theta = 0 \qquad v_\theta = -\frac{\partial\psi}{\partial r} = -2U_\infty\sin\theta + \frac{\Gamma}{2\pi R}$$

$-\Gamma = \oint \underline{V}\bullet d\underline{r} = \int_0^{2\pi} v_\theta r d\theta$, i.e., vortex strength is circulation

Next, consider the flow pattern as a function of Γ. To start lets calculate the stagnation points on the cylinder i.e.:

$$v_\theta = -2U_\infty\sin\theta + \frac{\Gamma}{2\pi R} = 0$$

$$\sin\theta = \frac{\Gamma}{4\pi U_\infty R} = \frac{K}{2U_\infty R} = \beta/2$$

Note: $K = \frac{\Gamma}{2\pi}$ $\beta = \frac{K}{U_\infty R}$

So, the location of stagnation point is function of Γ.

$\beta = \frac{K}{U_\infty R} = \frac{\Gamma}{2\pi U_\infty R}$	θ_s (stagnation point)
0 ($\sin\theta = 0$)	0,180
1($\sin\theta = 0.5$)	30,150
2 ($\sin\theta = 1$)	90
>2($\sin\theta > 1$)	Is not on the circle but where $v_r = v_\theta = 0$

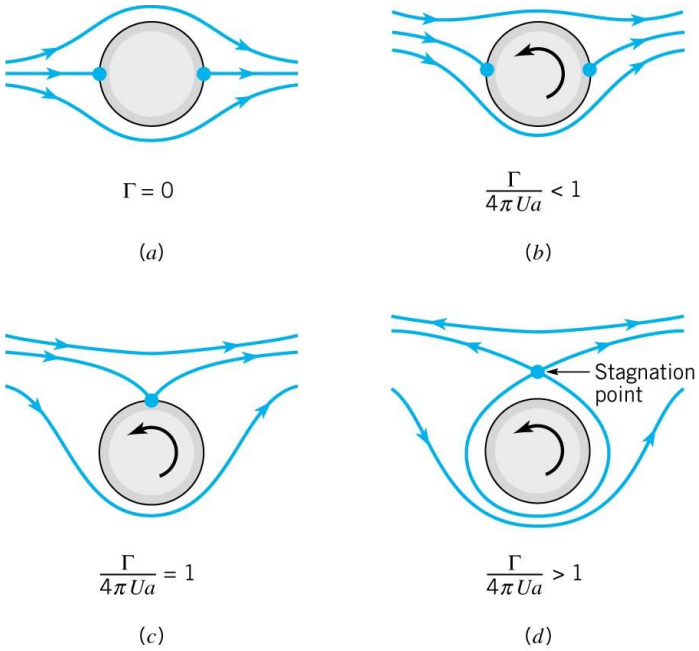

For flow patterns like above (except a), we should expect to have lift force in –y direction.

Summary of stream and potential function of elementary 2-D flows:

In Cartesian coordinates:

$u = \psi_y = \phi_x$

$v = -\psi_x = \phi_y$

In polar coordinates:

$v_r = \frac{\partial \phi}{\partial r} = \frac{1}{r}\frac{\partial \psi}{\partial \theta}$

$v_\theta = \frac{1}{r}\frac{\partial \phi}{\partial \theta} = -\frac{\partial \psi}{\partial r}$

Flow	ϕ	ψ
Uniform Flow	$U_\infty x$	$U_\infty y$
Source (m>0) Sink (m<0)	$m \ln r$	$m\theta$
Doublet	$\frac{\lambda \cos\theta}{r}$	$-\frac{\lambda \sin\theta}{r}$
Vortex	$K\theta$	$-K \ln r$
90 Corner flow	$1/2A(x^2 - y^2)$	Axy
Solid-Body rotation	Doesn't exist	$\frac{1}{2}\omega r^2$

These elementary solutions can be combined in such a way that the resulting solution can be interpreted to have physical significance; that is, represent the potential flow solution for various geometries. Also, methods for arbitrary geometries combine uniform stream with distribution of the elementary solution on the body surface.

Some combination of elementary solutions to produce body geometries of practical importance

Body name	Elemental combination	Flow Patterns
Rankine Half Body	Uniform stream+source	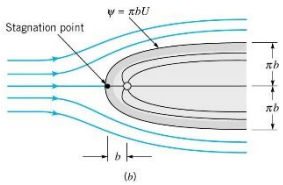
Rankine Oval	Uniform stream+source+sink	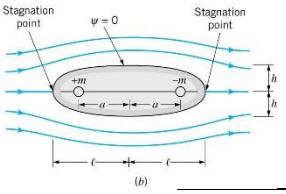
Kelvin Oval	Uniform stream+vortex point	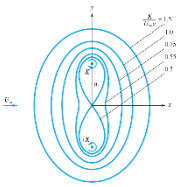
Circular Cylinder without circulation	Uniform stream+doublet	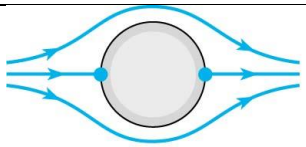
Circular Cylinder with circulation	Uniform stream+doublet+vortex	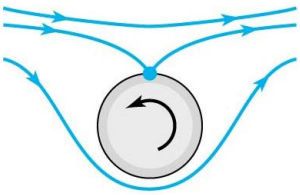 $\frac{\Gamma}{4\pi Ua} = 1$

Keep in mind that this is the potential flow solution and may not well represent the real flow especially in region of adverse px.

The Kutta – Joukowski lift theorem:

Since we know the tangential component of velocity at any point on the cylinder (and the radial component of velocity is zero), we can find the pressure field over the surface of the cylinder from Bernoulli's equation:

$$\frac{p}{\rho}+\frac{v_r^2}{2}+\frac{v_\theta^2}{2}=\frac{p_\infty}{\rho}+\frac{U_\infty^2}{2}$$

Therefore:

$$p=p_\infty+\frac{1}{2}\rho\left[U_\infty^2-\left\{2U_\infty\sin\theta-\frac{\Gamma}{2\pi R}\right\}^2\right]=\left(p_\infty+\frac{1}{2}\rho U_\infty^2-\frac{\rho\Gamma^2}{8\pi^2R^2}\right)-2\rho U_\infty^2\sin^2\theta+\frac{\rho U_\infty\Gamma}{\pi R}\sin\theta$$

$$=A+B\sin\theta+C\sin^2\theta$$

where

$$A=\left(p_\infty+\frac{1}{2}\rho U_\infty^2-\frac{\rho\Gamma^2}{8\pi^2R^2}\right)$$

$$B=\frac{\rho U_\infty\Gamma}{\pi R}$$

$$C=-2\rho U_\infty^2$$

Calculation of Lift: Let us first consider lift. Lift per unit span, L (i.e. per unit distance normal to the plane of the paper) is given by:

$$L=\int_{Lower}pdx-\int_{upper}pdx$$

On the surface of the cylinder, x = Rcosθ. Thus, dx = -Rsinθdθ, and the above integrals may be thought of as integrals with respect to θ. For the lower surface, θ varies between π and 2π. For the upper surface, θ varies between π and 0. Thus,

$$L=-R\int_\pi^{2\pi}\left(A+B\sin\theta+C\sin^2\theta\right)\sin\theta d\theta+R\int_\pi^0\left(A+B\sin\theta+C\sin^2\theta\right)\sin\theta d\theta$$

Reversing the upper and lower limits of the second integral, we get:

$$L=-R\int_0^{2\pi}\left(A+B\sin\theta+C\sin^2\theta\right)\sin\theta d\theta=-R\int_0^{2\pi}\left(A\sin\theta+B\sin^2\theta+C\sin^3\theta\right)d\theta=-BR\pi$$

Substituting for B ,we get:

$$L=-\rho u_\infty\Gamma$$

This is an important result. It says that clockwise vortices (negative numerical values of Γ) will produce positive lift that is proportional to Γ and the free stream speed with direction 90 degrees from the stream direction rotating opposite to the circulation. Kutta and

Joukowski generalized this result to lifting flow over airfoils. Equation $L = -\rho u_\infty \Gamma$ is known as the Kutta-Joukowski theorem.

Drag: We can likewise integrate drag forces. The drag per unit span, D, is given by:

$$D = \int_{Front} p dy - \int_{rear} p dy$$

Since y=Rsinθ on the cylinder, dy=Rcosθdθ. Thus, as in the case of lift, we can convert these two integrals over y into integrals over θ. On the front side, θ varies from 3π/2 to π/2. On the rear side, θ varies between 3π/2 and π/2. Performing the integration, we can show that

$$D = 0$$

This result is in contrast to reality, where drag is high due to viscous separation. This contrast between potential flow theory and drag is the **dÁlembert Paradox**.

The explanation of this paradox are provided by Prandtl (1904) with his boundary layer theory i.e. viscous effects are always important very close to the body where the no slip boundary condition must be satisfied and large shear stress exists which contributes the drag.

Lift for rotating Cylinder:

We know that $L = -\rho U_\infty \Gamma$ therefore:

$$C_L = \frac{L}{\frac{1}{2}\rho U_\infty^2 (2R)} = \frac{-\Gamma}{U_\infty R}$$

Define: $v_{\theta_{Average}} = \frac{1}{2\pi}\int_0^{2\pi} v_\theta d\theta = \frac{1}{2\pi}\left(\frac{\Gamma}{R}\right)$ Note: $\Gamma = \oint_c \underline{V}\cdot d\,\underline{s} = \oint_c \underline{V}_\theta \cdot d\,\underline{A} = \oint_c V_\theta R d\theta$

$$\Rightarrow C_L = \frac{2\pi}{U_\infty} v_{\theta_{averagfe}}$$

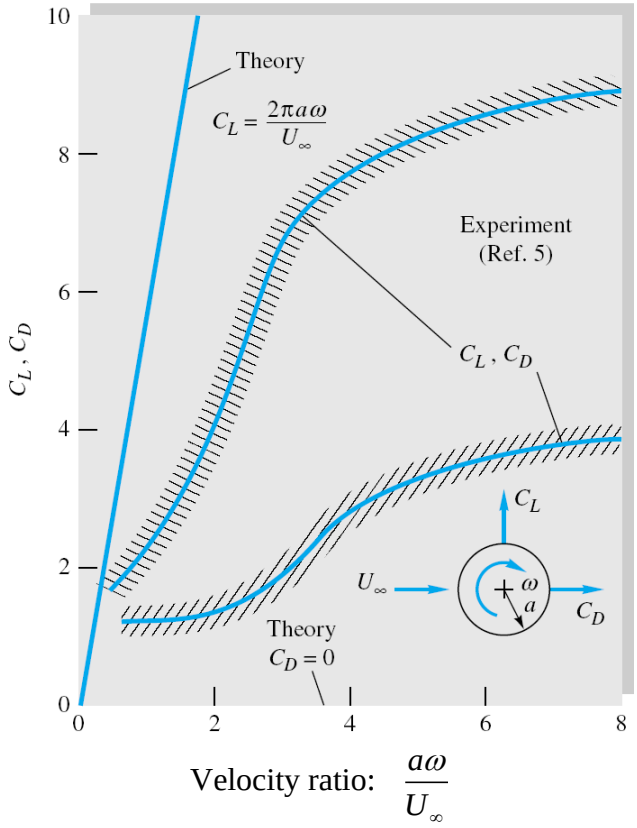

Theoretical and experimental lift and drag of a rotating cylinder

Experiments have been performed that simulate the previous flow by rotating a circular cylinder in a uniform stream. In this case $v_\theta = R\omega$ which is due to no slip boundary condition.

- Lift is quite high but not as large as theory (due to viscous effect ie flow separation)
- Note drag force is also fairy high

Flettner (1924) used rotating cylinder to produce forward motion.

27

Spindle Rotors Take the Place of Wings

by LAWRENCE E. ANDREWS

Using spindle shaped slotted rotors, the inventor expects to eliminate many of the difficulties formerly experienced with cylindrical rotors

ROTATING conical spindles instead of wings will provide the lifting surface for a new flight machine to be launched at Roosevelt Field this spring. While it is not the first machine projected with lifting rotors, it is the first using slotted, conical surfaces.

It is the invention of John G. Guest, while actual construction is being carried out by L. C. Popper, construction and designing engineer of New York city. A rotor-wing airplane was made a few years ago and was tried out on Long Island but its cylindrical type of rotor set up such an air disturbance that its control was seriously hampered.

This new ship makes use of the same general principle, but its mechanical execution is decidedly different. Laboratory tests have shown that it has a lifting power of 900 per cent greater than an equally surfaced conventional plane. In addition, it has the ability to land or take-off in very short distances —greatly like the Autogiro.

There are four spindles, two on each [illegible] in place of wings. The lift is [illegible]ed by the rotation of the spindles [illegible]g in the slip stream of the forward propeller, the rotation distorting and deflecting the air-stream downwards. Slots are hollowed out in the spindles which offer no resistance to the wind but are caught by the wind as they turn under. The slots serve to reduce the drag which disrupted control with former ships of this type.

There are three motors in the machine. One, a 90 horse power Cirrus engine provides power to the tractor propeller. Two others, with two cylinders each, provide power to the spindles. A universal throttle connects [illegible] carrier.

Recently the navy has placed lanaing-lights around the edges of the decks to facilitate night flying. Ability to fly at night is now a requirement, and much time is spent to keep the flyers in practice.

A plane about to land on the deck of the carrier.

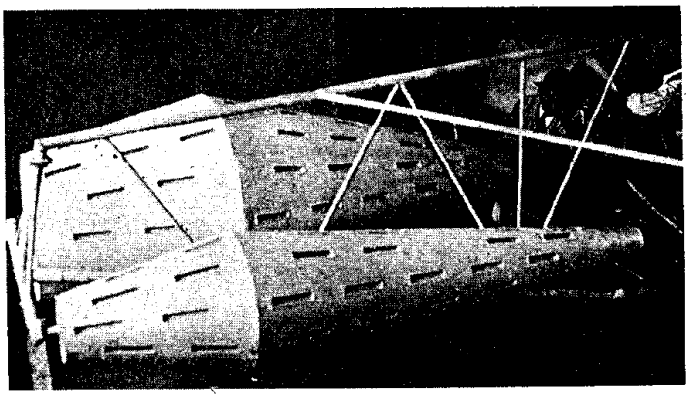

A close view of the curious rotors showing their shape and the slots cut into their surfaces. Note that the forward rotors are larger than those in the rear.

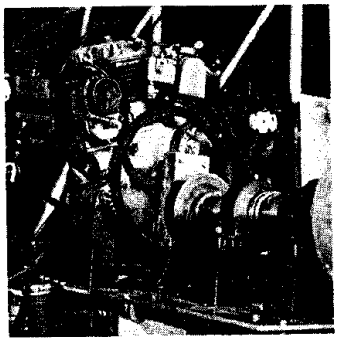

A detailed view of one of the small 2-cylinder engines employed for driving the forward spindles, together with the main bearings and gearing. End of spindle at right.

[illegible]
licenses.

10,780 airplanes were registered, including 3,227 unlicensed, having identification numbers only.

The licensed pilots included 532 women of which 433 were private and 42 were transport licenses.

New York has the greatest number of aircraft of all kinds, 1,227, with California second. On the other hand, California has the greatest number of licensed pilots leading with 3,327, and New York second.

Gliders were also listed. There were 1,270 gliders of which 89 were licensed. Licensed glider pilots numbered 267.

The report is interesting in that there is a decided increase in every item over those released for July of 1931.

with the pilot's seat. By speeding up or slowing down the rotor motors, lateral control is accomplished. Elevator and rudder controls govern longitudinal direction in the usual manner.

With full weight of pilot and fuel, the machine weighs 1,734 pounds. The cruising range is about 340 miles. It measures 23½ feet from tip to tip of spindles and is 18 feet long. The size compares favorably with that of the small training ship.

The spindles and their assembly weigh more than the wings in the ordinary airplane, but the gross weight is well under the figures set for light airplanes powered with the 90 horsepower Cirrus motors.

A New York manufacturing concern is financing the arrangements for the research and development work on the plane. They plan to manufacture the odd looking craft after the preliminary field and flight tests are made.

This machine is an excellent example of many similar attempts now being made toward producing a direct lift wingless ship. There is undoubtedly a great field for wingless ships of this same general type and inventors will make no mistake in experimenting along these lines.

From experiments made to date, it is evident that the weight of a machine can be supported with a smaller expenditure of power than where wings are employed. Very little power is taken by the rotors, and this fact alone justifies the additional complication.

Whether it will pay to employ auxiliary wings for safety in case of engine failure, it is difficult to say, but in such a case the use of a parachute is an alternative.

18 28

One very important improvement on wing construction, and one that has proved very practicable in service, is the "slotted wing" invented by Handley-Page. This device very materially increases the speed range of a ship by varying the lift, and by allowing higher angles of attack than possible with a plain wing.

Essentially, this invention consists of a metal guide placed along the entering edge of the wing. This so controls the flow of air over the top surface of the wing that the air does not break away from the wing or "burble" until very high angles of attack are attained. The slots are controlled automatically or manually, depending upon conditions.

However, it has been discovered that the wing "slots" are much more effective if an aileron is installed along the whole length of the trailing edge. At high angles, this hinged rear flap is depressed, and by this means even a greater lift is obtained at low speeds than with the slots alone. The writer has witnessed a ship of this type taking off and landing easily inside of a 100 foot circle. In a 15 m.p.h. breeze it hovered directly over one spot.

Handley-Page also instituted another innovation in wing construction which departs entirely from the standard wing. Essentially, it consists of a series of short streamline blades built into a unit, much after the manner of a Venetian blind or lattice. Each of these streamline blades is placed progressively at a flatter angle as we approach the trailing edge of the structure, and in this way, the whole area of the wing is utilized effectively.

Next, in the development of wingless wings, is the cellule construction of the "Vacuplane," described in the November issue of POPULAR AVIATION. This, it will be remembered, consisted of a short stubby cell carried over the fuselage, the upper surface of the cell consisting of rods or slats. It is claimed that this arrangement so greatly decreases the pressure on the top of the cell that a very much greater speed range is obtained.

Helicopters, of some sort or other, have always been with us. Few of them have shown much indication of success until the coming of the Autogiro, which in general, belongs to the helicopter family. Helicopters, or machines equipped with lifting propellers, look nice on paper but they have more inherent defects than wings. True, they have the advantage of landing and taking off at near zero speed, but they are mechanically complicated.

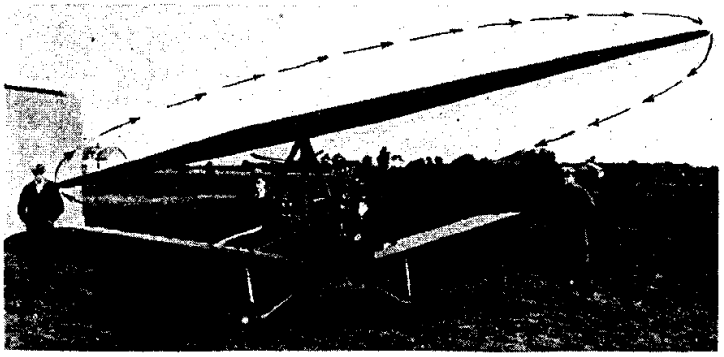

The Stauffer "Gyroplane," showing the single blade rotor which turns only on landing or take-off.

We only look at their one advantage, that is of slow landing, but fail to see at the same time that their top speed is limited. When we simmer the whole thing down into a nutshell, the speed range is not much greater, and usually less than an airplane.

In the point of low landing speed, a helicopter or lifting screw type has little advantage over an equally standard loaded wing, and still less advantage over a slotted wing type. The Autogiro, for example, has a top speed of about 100 m.p.h. but with the same top speed and loading, an airplane can land nearly as slowly.

Now, a helicopter type known as the Gyroplane, has recently been developed. It is apparently based upon a more logical principle than those that have gone before it. This is a combination of an airplane and helicopter, with the rotor used as an auxiliary to the wing.

When taking off, flying at slow horizonal speed, or in landing, the lifting propeller revolves and assists the wings. However, when the plane is to fly at high speed, the lifting propeller or rotor is stopped so that flight is now maintained by the wings alone.

Thus, if the wings are of the high speed type, this gives a tremendous speed range. It has a good gliding angle with a dead engine. This ship will probably range from a low speed of 15 m.p.h. to a high speed of about 145 m.p.h.

And now we get down to the so-called "rotor" or cylinder type of lift, which as you probably know, consists of a large diameter rotating cylinder projecting out on both sides of the fuselage. When the rotors are not turning, the air-stream splits equally around the cylinders and there is no lifting force exerted.

However, when the cylinders revolve the air-stream is twisted about in such a way that the pressure is higher on one side of the cylinder than on the other, thus producing the lift. Very little power is required to produce the rotation, and the cylinders can either be driven directly by the engine or else through the action of the wind-stream. A small amount of cylinder surface produces a remarkable amount of lift.

Now, this plain rotor is entirely ineffective when the engine stops, hence the machine will drop suddenly as soon as the engine cuts out. To avoid this difficulty, it is safest to combine the rotor with a wing in such a way that the wing will always be available alone for dead engine landings or high speed operation.

One experimenter, Mr. Ray Thompson, who has recently come into our notice, has designed a new application of the rotor and wing. He has done quite a bit of experimenting with large models and has obtained quite remarkable results. This general class of lifting device, in my opinion, is the first step in the complete elimination of wings—far more practical than any possible helicopter arrangement. We hereby quote from a letter by Mr. Thompson on the subject:

"The rotor wing model had a span of 38 inches and a length of 42 inches, with a wing area of 360 square inches. With the rotors turning, it carried a load of 9.5 pounds to a height of 18 feet, the rotor being driven by an electric motor. This model had no propeller for pulling it forward, but was

(*Continued on page* 58)

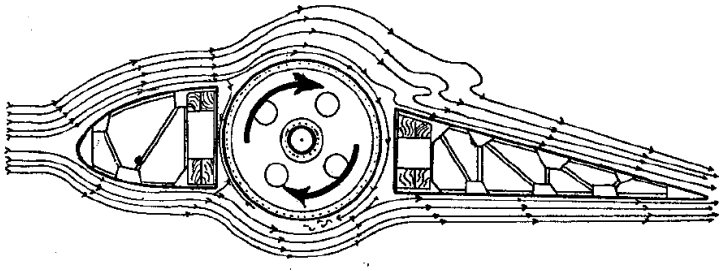

The Thompson Rotor-wing with the rotor imbedded in a deep wing section. Lines show air distribution.

8.4 Method of Images

The method of image is used to model "slip" wall effects by constructing appropriate image singularity distributions.

Plane Boundaries:

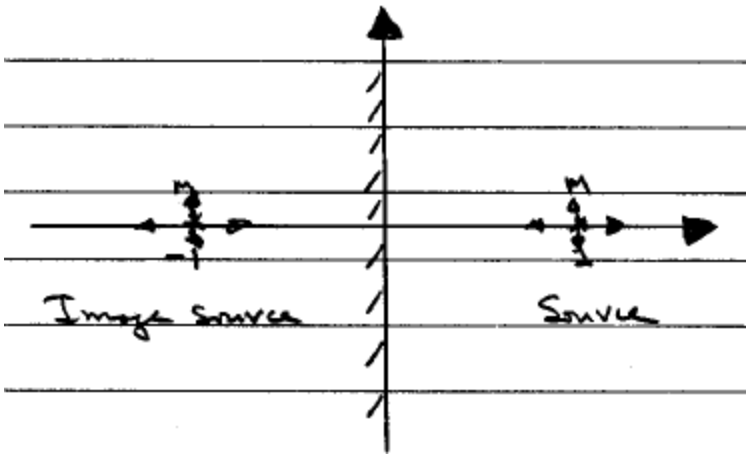

2-D: $\Phi = \frac{m}{2}\left(ln[(x-1)^2 + y^2]^{\frac{1}{2}} + ln[(x+1)^2 + y^2]^{\frac{1}{2}}\right)$

Similar results can be obtained for dipoles and vortices:

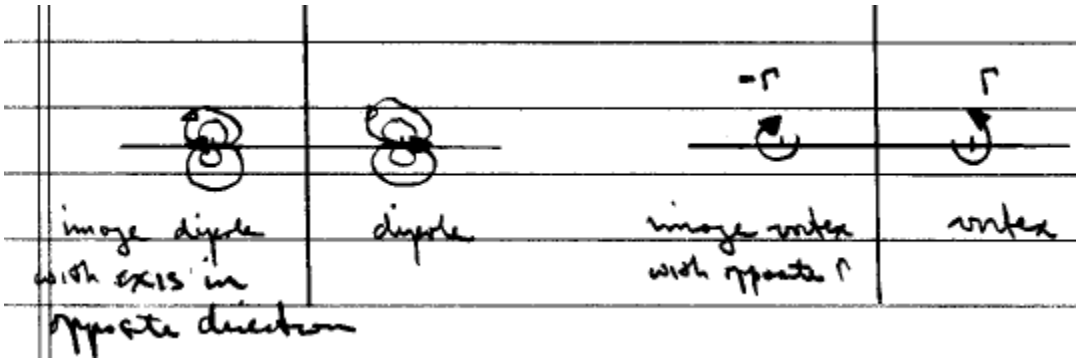

Spherical and Curvilinear Boundaries:

The results for plane boundaries are obtained from consideration of symmetry. For spherical and circular boundaries, image systems can be determined from the Sphere & Circle Theorems, respectively. For example:

Flow field	Image System
Source of strength M at c outside sphere of radius a, c>a	Sources of strength ma/c at a^2/c and line sink of strength m/a extending from center of sphere to a^2/c
Dipole of strength μ at l outside sphere of radius a, $l>a$	dipole of strength $-a^3\mu/l$ at $-a^2/l$
Source of strength m at b outside circle of radius a, b>a	equal source at a^2/b and sink of same strength at the center of the circle

Multiple Boundaries:

The method can be extended for multiple boundaries by using successive images.

(1) For example, the solution for a source equally spaced between two parallel planes

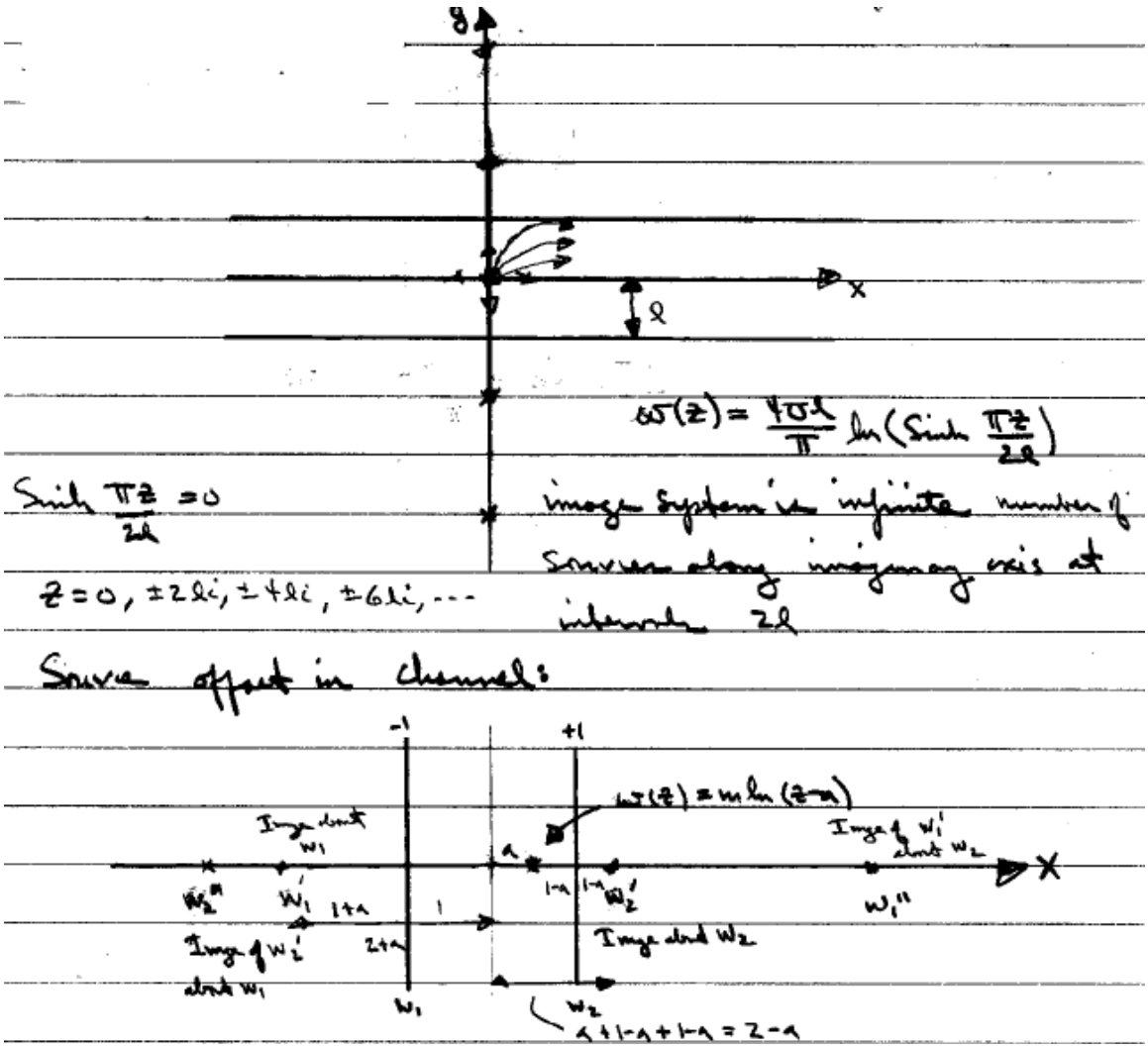

$$w(z) = m \sum_{m=0,\pm1,\pm2,\ldots} \left[\ln\left[z-(4n+a)\right] + \ln\left[z-(4n+2-a)\right]\right]$$

$$= m\left[\ln(z-a) + \ln(z-2+a) + \ln(z-4+a) + \ln(z-6+a) + \ln(z+4-a) + \ln(z+2+a) + \ldots\right]$$

(2) As a second example of the method of successive images for multiple boundaries consider two spheres A and B moving along a line through their centers at velocities U_1 and U_2, respectively:

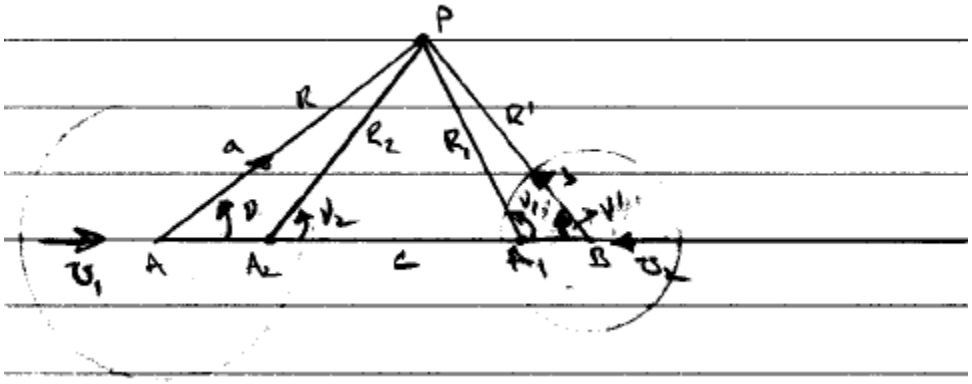

Consider the kinematic BC for A:

$$F(x,t) = (x - yt)^2 + y^2 + z^2 - a^2$$

$$\frac{DF}{Dt} = 0 \Rightarrow \underline{V} \cdot \hat{e}_R = U_1 \hat{k} \cdot \hat{e}_R \text{ or } \phi_R = U_1 \cos\nu$$

where $\varphi = -\frac{\Delta}{R^2}\cos\nu$, $\phi_R = -\frac{2\Delta}{R^3}\cos\nu \Rightarrow \Delta = \frac{Ua^3}{2}$ for single sphere

Similarly for B→ $\phi_R = U_2 \cos\nu'$

This suggests the potential in the form

$$\varphi = U_1\varphi_1 + U_2\varphi_2$$

where ϕ_1 and ϕ_2 both satisfy the Laplace equation and the boundary condition:

$$\left(\frac{\partial\phi_1}{\partial R}\right)_{R=a} = \cos\nu, \ \left(\frac{\partial\phi_1}{\partial R'}\right)_{R'=b} = 0 \qquad (*)$$

$$\left(\frac{\partial\phi_2}{\partial R}\right)_{R=a} = 0, \ \left(\frac{\partial\phi_2}{\partial R'}\right)_{R'=b} = \cos\nu' \qquad (**)$$

ϕ_1 = potential when sphere A moves with unit velocity towards B, with B at rest
ϕ_2 = potential when sphere B moves with unit velocity towards A, with A at rest

If B were absent.

$$\phi_1 = -\frac{a^3}{2R^2}\cos\nu = -\frac{\Delta_0}{R^2}\cos\nu,\ \Delta_0 = \frac{a^3}{2}$$

but this does not satisfy the second condition in (*). To satisfy this, we introduce the image of Δ_0 in B, which is a doublet Δ_1 directed along BA at A_1, the inverse point of A with respect to B. This image requires an image Δ_2 at A_2, the inverse of A_1 with respect to A, and so on. Thus we have an infinite series of images A_1, A_2, … of strengths $\Delta_1, \Delta_2, \Delta_3$ etc. where the odd suffixes refer to points within B and the even to points within A.

Let $f_n = AA_n$ & $AB = c$

$$f_1 = c - \frac{b^2}{c},\ f_2 = \frac{a^2}{f_1},\ f_3 = c - \frac{b^2}{c - f_2},\ldots$$

$$\Delta_1 = \Delta_0\left(-\frac{b^3}{c^3}\right),\ \Delta_2 = \Delta_1\left(-\frac{a^3}{f_1{}^3}\right),\ \Delta_3 = \Delta_2\left(-\frac{b^3}{(c-f_2)^3}\right),\ldots$$

where Δ_1 = image dipole strength, Δ_0 = dipole strength $\times \frac{\text{radius}^3}{\text{sistance}^3}$

$\phi_1 = -\frac{\Delta_0\cos\nu}{R^2} - \frac{\Delta_1\cos\nu_1}{R_1{}^2} - \frac{\Delta_2\cos\nu_2}{R_2{}^2} - \ldots$ with a similar development procedure for ϕ_2. Although exact, this solution is of unwieldy form. Let's investigate the possibility of an approximate solution which is valid for large c (i.e. large separation distance)

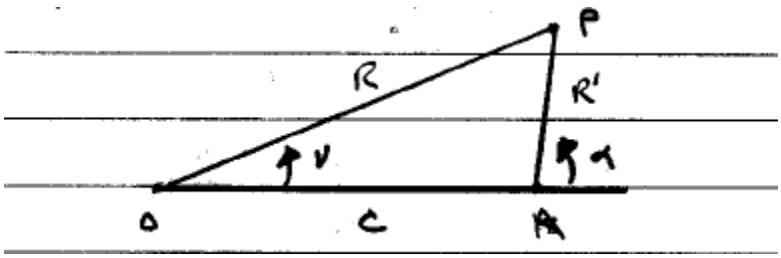

$$R'^2 = R^2 + c^2 - 2cr\cos\nu = R^2\left(1 - \frac{2c}{R}\cos\nu + \frac{c^2}{R^2}\right)$$

$$\frac{1}{R'} = \frac{1}{R}\left[1 - 2\frac{c}{R}\cos\nu + \frac{c^2}{R^2}\right]^{-\frac{1}{2}} = \frac{1}{c}\left[1 - 2\frac{R}{c}\cos\nu + \frac{R^2}{c^2}\right]^{-\frac{1}{2}}$$

Considering the former representation first defining $\mu = \frac{c}{R}$ and $u = \cos\upsilon$

$$\frac{1}{R'} = \frac{1}{R}\left[1 - 2u\mu + \mu^2\right]^{-\frac{1}{2}}$$

By the binomial theorem valid for $|x| < 1$

$$(1-x)^{-\frac{1}{2}} = \alpha_0 + \alpha_1 x + \alpha_2 x^2 + \alpha_3 x^3 + \cdots,\ \alpha_0 = 1 \text{ and } \alpha_n = \frac{1\cdot 3\cdot (2n-1)}{2\cdot 4\cdot 2n}$$

Hence if $\left|2u\mu - \mu^2 < 1\right|$

$$[\ ]^{-\frac{1}{2}} = \alpha_0 + \alpha_1\left(2u\mu - \mu^2\right) + \alpha_2(\ )^2 + \cdots = P_0(u) + P_1(u)\mu + P_2(u)\mu^2$$

After collecting terms in powers of μ, where the P_n are Legendre functions of the first kind (i.e. Legendre polynomials which are Legendre functions of the first kind of order zero). Thus,

$$R < C: \frac{1}{R'} = \frac{1}{c} + \frac{R}{c^2}P_1(\cos\nu) + \frac{R^2}{c^3}P_2(\cos\nu) + \cdots$$

$$R > C: \frac{1}{R'} = \frac{1}{R} + \frac{c}{R^2}P_1(\cos\nu) + \frac{c^2}{R^3}P_2(\cos\nu) + \cdots$$

Next, consider a doublet of strength Δ at A

$$\phi = -\frac{\Delta\cos\alpha}{R'^2} = \frac{-\Delta\left(R\cos\nu - c\right)}{\left(R^2 + c^2 - 2cR\cos\nu\right)^{\frac{3}{2}}} = -\Delta\frac{\partial}{\partial c}\left[\frac{1}{\left(R^2 + c^2 - 2cR\cos\nu\right)^{\frac{1}{2}}}\right]$$

Thus,

$$R < c: \phi = \frac{-\Delta\cos\alpha}{R'^2} = \Delta\left[\frac{1}{c^2} + \frac{2RP_1(\cos\nu)}{c^3} + \frac{3R^2P_2(\cos\nu)}{c\nu} + \cdots\right]$$

$$R > c: \phi = -\Delta\left[\frac{1}{R^2}P_1(\cos\nu) + \frac{2c}{R^3}P_2(\cos\nu) + \frac{3c^2}{R^4}P_3(\cos\nu) + \cdots\right]$$

Going back to the two sphere problem. If B were absent

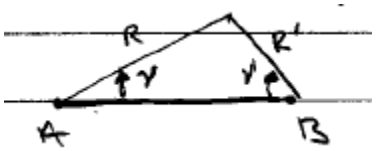

$$\phi_1 = -\frac{a^3}{2R^2}\cos\nu$$

using the above expression for the origin at B and near B $\left(\frac{R'}{c} < 1\right)$, R→R', $\nu \to \nu'$

$$\phi = -\frac{a^3}{2R^2}\cos\nu = -\left[\frac{1}{2}\frac{a^3}{c^2} + \frac{a^3R'P_1(\cos\nu)}{c^3} + \cdots\right]$$

$$\phi_R = \frac{-a^3\cos\nu}{c^3} + \cdots$$

which can be cancelled by adding a term to the first approximation, i.e.

$$\phi_1 = -\frac{1}{2}\frac{a^3\cos\nu}{R^2} - \frac{1}{2}\frac{a^3b^3}{c^3}\frac{\cos\nu'}{R'^2}$$

to confirm this

$$\phi_1 = -\frac{1}{2}\frac{a^3}{c^2} - \frac{a3R'\cos\nu'}{c^3} - \frac{1}{2}\frac{a^3b^3}{c^3}\frac{\cos\nu}{R}$$

$$\frac{\partial\phi_1}{\partial R'}(R' = b) = -\frac{a^3\cos\nu'}{c^3} + \frac{a^3b^3}{c^3}\frac{\cos\nu'}{R'^3} = 0 + hot$$

Similarly, the solution for f2 is

$$\phi_2 = -\frac{1}{2}\frac{b^3\cos\nu'}{R'^2} - \frac{1}{2}\frac{a^3b^3}{c^3}\frac{\cos\nu}{R^2}$$

These approximate solutions are converted to $\mathrm{O}\left(c^{-3}\right)$.

To find the kinetic energy of the fluid, we have

$$K = -\frac{1}{2}\rho\left[\int_{S_A}\phi\phi_n dS + \int_{S_B}\phi\phi_n dS\right]$$

$$K = \frac{1}{2}\left[A_{11}U_1^2 + A_{12}U_1U_2 + A_{22}U_2^2\right] = -\frac{\rho}{2}\int_{S_A+S_B}\phi\phi_n dS$$

$$A_{11} = -\rho\int_A \phi_1\frac{\partial\phi_1}{\partial n}dS_A,\ A_{22} = -\rho\int_B \phi_2\frac{\partial\phi_2}{\partial n}dS_B,\ A_{12} = -\rho\int_A \phi_2\frac{\partial\phi_1}{\partial n}dS_A = -\rho\int_B \phi_1\frac{\partial\phi_1}{\partial n}dS_B$$

where $dS = 2\pi R^2\sin\upsilon d\upsilon$

$A_{11} = \frac{2}{3}\pi a^3\rho,\ A_{12} = \frac{2\pi a^3b^3}{c^3}\rho,\ A_{22} = \frac{2}{3}\pi b^3\rho,$

$K = \frac{1}{4}M'_1U_1^2 + \frac{2\pi a^3b^3\rho}{c^3}U_1U_2 + \frac{1}{4}M'_2U_2^2$: using the approximate form of the potentials

where $\frac{1}{4}M'_1U_1^2, \frac{1}{4}M'_2U_2^2$: masses of liquid displaced by sphere.

8.5 Complex variable and conformal mapping

This method provides a very powerful method for solving 2-D flow problems. Although the method can be extended for arbitrary geometries, other techniques are equally useful. Thus, the greatest application is for getting simple flow geometries for which it provides closed form analytic solution which provides basic solutions and can be used to validate numerical methods.

Function of a complex variable

Conformal mapping relies entirely on complex mathematics. Therefore, a brief review is undertaken at this point.

A complex number *z* is a sum of a real and imaginary part; $z =$ real + i imaginary

The term *i*, refers to the complex number $i = \sqrt{-1}$

so that; $$i = \sqrt{-1}, \quad i^2 = -1, \quad i^3 = -i, \quad i^4 = 1$$

Complex numbers can be presented in a graphical format. If the real portion of a complex number is taken as the abscissa, and the imaginary portion as the ordinate, a two-dimensional plane is formed.

z = real +i imaginary = x + iy

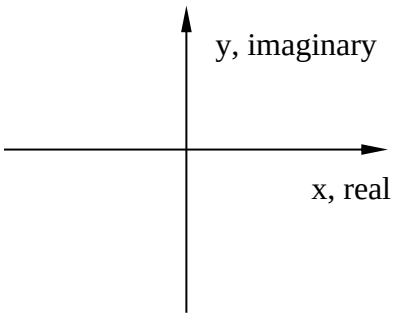

-A complex number can be written in polar form using Euler's equation;

$$z = x + iy = re^{i\theta} = r(\cos\theta + i\cdot\sin\theta)$$

Where: $r^2 = x^2 + y^2$

- Complex multiplication: $z_1 \cdot z_2 = (x_1+iy_1)(x_2+iy_2) = (x_1x_2 - y_1y_2) + i(x_1y_2 + y_1x_2)$

$$= r_1e^{i\theta_1} \cdot r_2e^{i\theta_2} = r_1r_2 \cdot e^{i(\theta_1+\theta_2)}$$

- Conjugate: $z = x + iy \quad \bar{z} = x - iy \; z.\bar{z} = x^2 + y^2$

-Complex function:

$$\boldsymbol{w(z) = f(z) = \phi(x,y) + i\psi(x,y)}$$

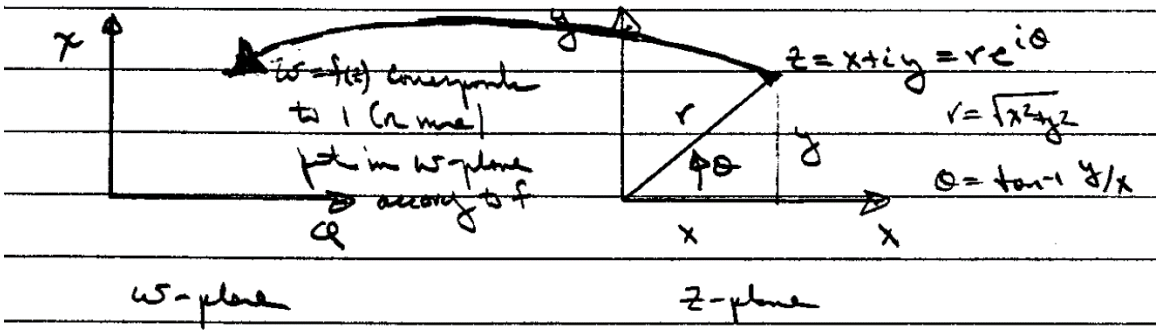

If function w(z) is differentiable for all values of z in a region of z plane is said to be regular and analytic in that region. Since a complex function relates two planes, a point can be approached along an infinite number of paths, and thus, in order to define a unique derivative f(z) must be independent of path.

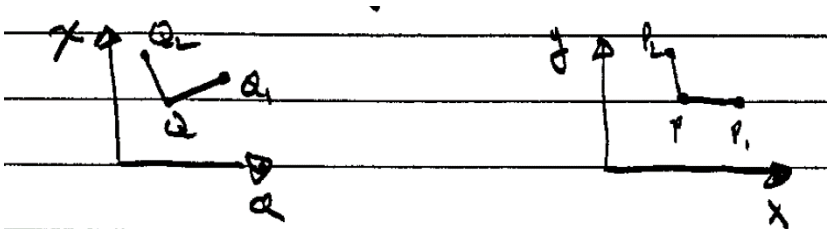

$$PP1(\delta y = 0): \quad \frac{\delta w}{\delta z} = \frac{w_1 - w}{z_1 - z} = \frac{\phi_1 + i\psi_1 - (\phi + i\psi)}{x_1 - x}$$

$$\Rightarrow \left.\frac{dw}{dz}\right|_1 = \phi_x + i\psi_x$$

$$Note: \; w_1 = \phi_1(x + \delta x, y) + i\psi_1(x + \delta x, y)$$

$$PP2(\delta x = 0): \quad \frac{\delta w}{\delta z} = \frac{w_2 - w}{z_2 - z} = \frac{\phi_2 + i\psi_2 - (\phi + i\psi)}{i(y_2 - y)}$$

$$\Rightarrow \left.\frac{dw}{dz}\right|_2 = -i\phi_y + \psi_y$$

For $\frac{dw}{dz}$ to be unique and independent of path:

$\phi_x = \psi_y \; and \; -\phi_y = \psi_x$ Cauchy Riemann Eq.

Recall that the velocity potential and stream function were shown to satisfy this relationship as a result of their othogonality. Thus, complex function $w = \phi + i\psi$ represents 2-D flows. $\phi_{xx} = \psi_{yx} \quad \phi_{yy} = -\psi_{xy}$ i.e. $\phi_{xx} + \phi_{yy} = 0$ and similarly for ψ. Therefore if analytic and regular also harmonic, i.e., satisfy Laplace equation.

Application to potential flow

$w(z) = \phi + i\psi$ Complex potential where ϕ: velocity potential, ψ: stream function

$\frac{dw}{dz} = \phi_x + i\psi_x = u - iv = \left(u_r - iu_\theta\right)e^{-i\theta}$ Complex velocity

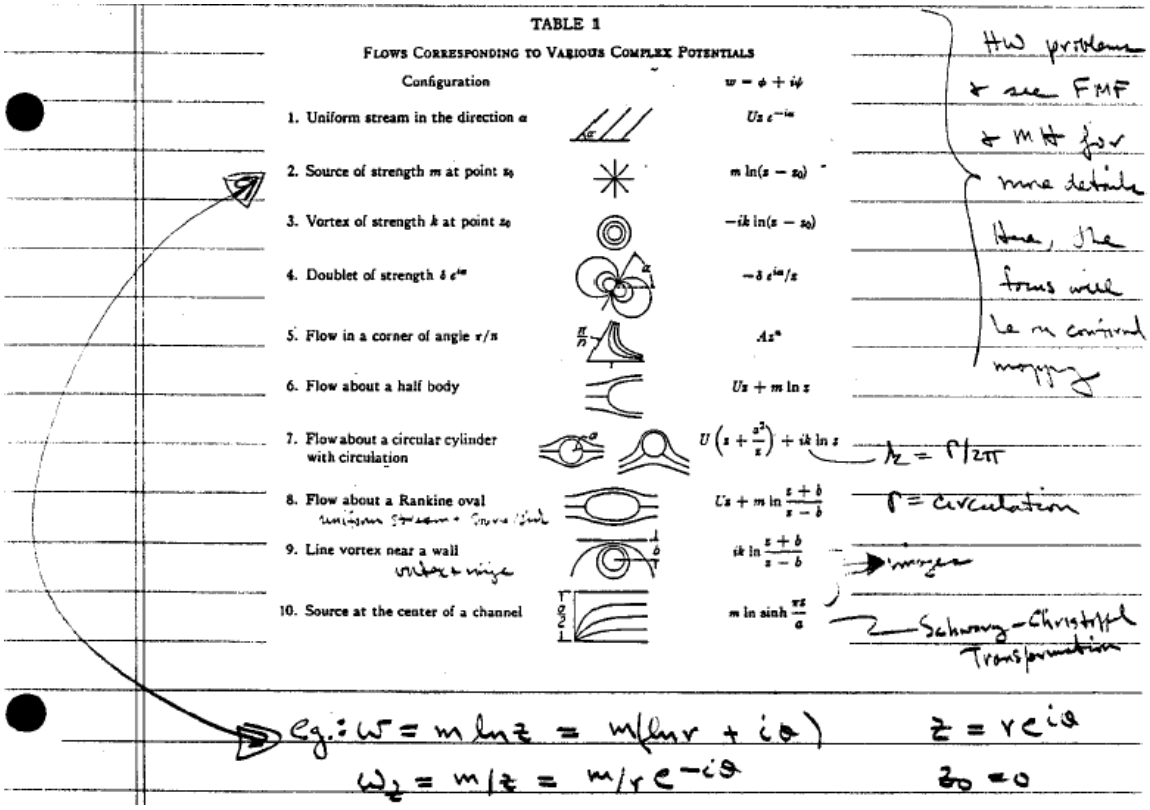

TABLE 1

FLOWS CORRESPONDING TO VARIOUS COMPLEX POTENTIALS

Configuration	$w = \phi + i\psi$
1. Uniform stream in the direction α	$Uz\,e^{-i\alpha}$
2. Source of strength m at point z_0	$m \ln(z - z_0)$
3. Vortex of strength k at point z_0	$-ik \ln(z - z_0)$
4. Doublet of strength $\delta\, e^{i\alpha}$	$-\delta\, e^{i\alpha}/z$
5. Flow in a corner of angle π/n	Az^n
6. Flow about a half body	$Uz + m \ln z$
7. Flow about a circular cylinder with circulation	$U\left(z + \frac{a^2}{z}\right) + ik \ln z$
8. Flow about a Rankine oval	$Uz + m \ln \frac{z+b}{z-b}$
9. Line vortex near a wall	$ik \ln \frac{z+b}{z-b}$
10. Source at the center of a channel	$m \ln \sinh \frac{\pi z}{a}$

$r'e^{i\theta'} = \rho r e^{i(\theta+\alpha)}$ where $r' = \rho r$ (magnification) and $\theta' = \theta + \alpha$ (rotation)

→Triangle about z_0 is transformed into a similar triangle in the ζ-plane which is magnified and rotated.

Implication:

-Angles are preserved between the intersections of any two lines in the physical domain and in the mapped domain.

-The mapping is one-to-one, so that to each point in the physical domain, there is one and only one corresponding point in the mapped domain.

For these reasons, such transformations are called conformal.

Usually the flow-field solution in the ζ-plane is known:

$$W(\varsigma) = \Phi(\xi,\eta) + i\Psi(\xi,\eta)$$

Then

$$w(z) = W\left(f(z)\right) = \phi(x,y) + i\psi(x,y) \text{ or } \phi = \Phi \,\&\, \psi = \Psi$$

Conformal mapping

The real power of the use of complex variables for flow analysis is through the application of conformal mapping: techniques whereby a complicated geometry in the physical z-domain is mapped onto a simple geometry in the ζ-plane (circular cylinder) for which the flow-field solution is known. The flow-field solution in the z-plane is obtained by relating the ζ-plane solution to the z-plane through the conformal transformation ζ=f(z) (or inverse mapping z=g(ζ)).

Before considering the application of the technique, we shall review some of the more important properties and theorems associated with it.

Consider the transformation,
ζ=f(z) where f(z) is analytic at a regular point Z_0 where f'(z_0)≠0
δζ= f'(z_0) δz
$\delta\varsigma = r'e^{i\theta'}$, $\delta z = re^{i\theta}$, $f'(z_0) = \rho e^{i\alpha}$

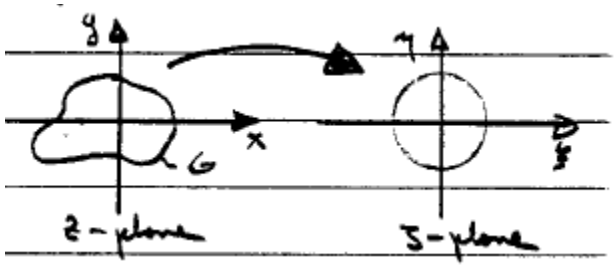

→The streamlines and equipotential lines of the ζ-plane (Φ, Ψ) become the streamlines of equipotential lines of the z-plane (ϕ, ψ).

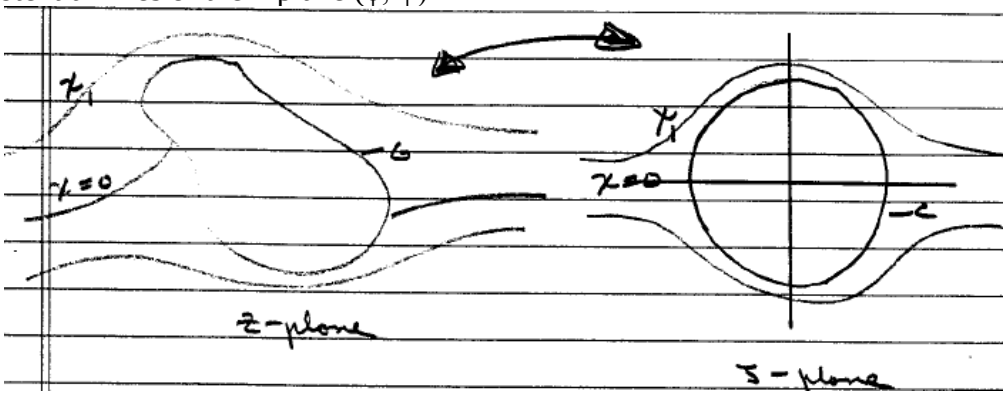

→ $\nabla_z^2\varphi = \nabla_\varsigma^2\phi = 0$
$\nabla_z^2\psi = \nabla_\varsigma^2\psi = 0$ i.e. Laplace equation in the z-plane transforms into Laplace equation is the ζ-plane.

The complex velocities in each plane are also simply related

$$\frac{dw}{dz} = \frac{dw}{d\varsigma}\frac{d\varsigma}{dz} = \frac{dw}{d\varsigma} f'(z)$$

$$\frac{dw}{dz}(z) = u - iv = (U - iV) f'(z) = \frac{dW}{d\zeta}(\zeta = f(z))$$

i.e. velocities in two planes are proportional.

Two independent theorems concerning conformal transformations are:

(1) Closed curves map to closed curves
(2) Rieman mapping theorem: an arbitrary closed profile can be mapped onto the unit circle.

More theorems are given and discussed in AMF Section 43. Note that these are for the interior problems, but are equally valid for the exterior problems through the inversion mapping.

Many transformations have been investigated and are compiled in handbooks. The AMF contains many examples:

1) Elementary transformations:

a) linear: $w = \frac{az+b}{cz+d}, ad - bc \neq 0$

b) corner flow: $w = Az^n$

c) Jowkowsky: $w = \varsigma + c^2/\varsigma$

d) exponential: $w = e^n$

e) $w = z^s$, s irational

2) Flow field for specific geometries

a) circle theorem
b) flat plate
c) circular arc
d) ellipse
e) Jowkowski foils
f) ogive (two circular areas)
g) Thin foil theory [solutions by mapping flat plate with thin foil BC onto unit circle]
h) multiple bodies

3) Schwarz-Cristoffel mapping
4) Free-streamline theory

The techniques of conformal mapping are best learned through their applications. Here we shall consider corner flow.

A simple example: Corner flow

1. In ζ-plane, let $W(\varsigma) = \varsigma$ i.e. uniform stream
2. Say→ $\varsigma = f(z) = z^{\pi/\theta}$
3. $w(z) = W(f(z)) = z^{\pi/\theta}$ i.e. corner flow

Note that 1-3 are unit uniform stream.

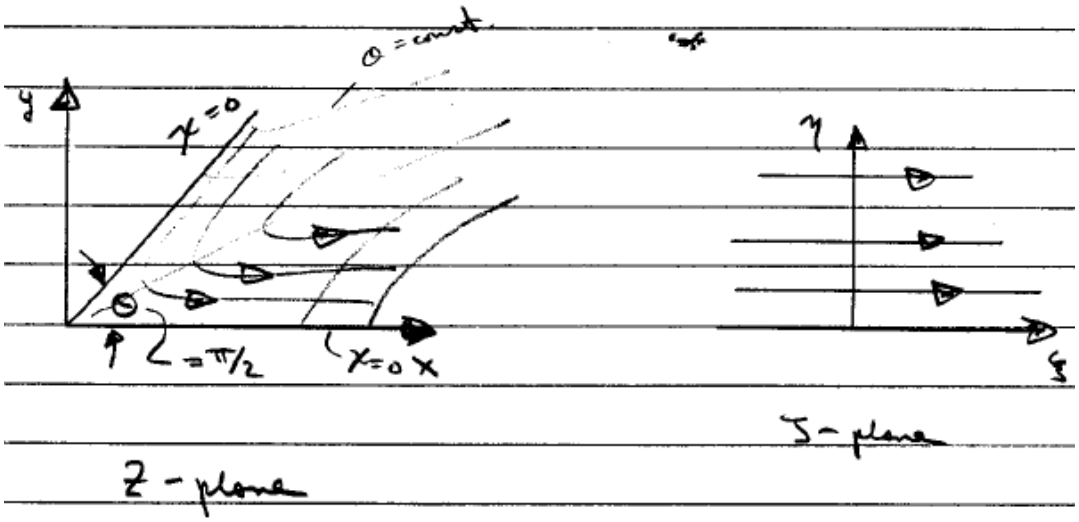

$$w(z) = Uz^n = UR^n \cos\theta + iUR^n \sin n\theta \text{, where } z = \mathrm{Re}^{i\theta}$$

i.e. $\phi = UR^n \cos n\theta$, $\psi = UR^n \sin n\theta$

$\psi = UR^n \sin n\theta$ =const.=streamlines

$\phi = UR^n \cos n\theta$ =const.=equipotentials

$$\frac{dw}{dz} = \frac{dW}{d\varsigma}\frac{d\varsigma}{dz} = nUz^{n-1} = nUR^{n-1}e^{i(n-1)\theta} = (nUR^{n-1}\cos n\theta + inUR^{n-1}\sin n\theta)e^{-i\theta}$$

$$= (u_r - iu_\theta)e^{-i\theta}$$

$$u_r = nUR^{n-1}\cos n\theta$$

$$u_\theta = -nUR^{n-1}\sin n\theta$$

$$0 < \theta < \left(\pi/2n\right) \rightarrow u_r > 0,\ u_\theta < 0$$

$$\left(\pi/2n\right) < \theta < \left(\pi/n\right) \rightarrow u_r < 0,\ u_\theta < 0$$

i.e. $w(z) = Uz^n$

represents corner flow: n=1→uniform stream, n=2→90° corner

8.6 Introduction to Surface Singularity methods (also known as Boundary Integral and Panels Methods)

Next, we consider the solution of the potential flow problem for an arbitrary geometry. Consider the BVP for a body of arbitrary geometry fixed in a uniform stream of an inviscid, incompressible, and irrotational fluid.

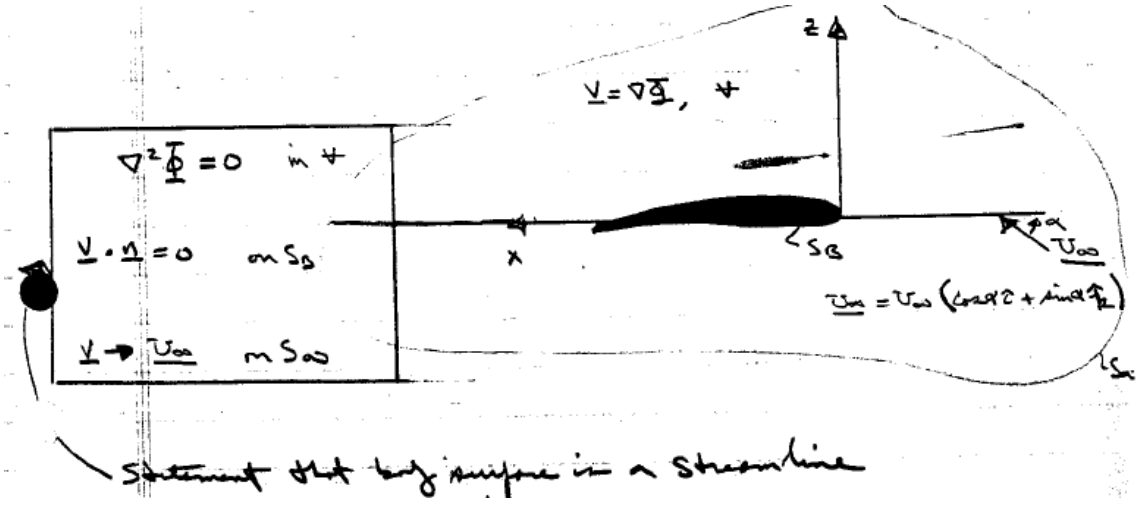

The surface singularity method is founded on the symmetric form of Greens theorem and what is known as Greens function.

$$\int_V \left(G\nabla^2\Phi - \Phi\nabla^2 G\right)dV = \int_{\sum S=S_\infty+S_B+S_S} \left(G\frac{\partial\Phi}{\partial n} - \Phi\frac{\partial G}{\partial n}\right)dS \qquad (1)$$

where Φ and G are any two scalar field in V (control volume bounded by s infinity S body and S inserted to render the domain simply connected) and for our application.
Φ= velocity potential
G= Green's function

Say,
$\nabla^2 G = -\delta(\underline{x} - \underline{x_0})$ in V+V' (i.e. entire domain) where δ is the Dirac delta function.
G→0 on S_∞

Solution for G (obtained Fourier Transforms) is: $G = \ln|\underline{r}|$, $|r| = |\underline{x} - \underline{x_0}|$, i.e. elementary 2-D source at $\underline{x} = \underline{x_0}$ of unit strength, and (1) becomes

$$\Phi = \int_{\sum S=S_B} \left(G\frac{\partial\Phi}{\partial n} - \Phi\frac{\partial G}{\partial n}\right)dS$$

First term in integrand represents source distribution and second term dipole distribution, which can be transformed to vortex distribution using integration by parts. By extending the definition of Φ into V' it can be shown that Φ can be represented by distributions of sources, dipoles or vortices, i.e.

$$\Phi = \sum \int_{S=S_B} \sigma G dS : \text{source distribution, } \sigma : \text{source strength}$$

or

$$\Phi = \sum \int_{S=S_B} \lambda \frac{\partial G}{\partial n} dS : \text{dipole distribution, } \lambda : \text{dipole strength}$$

Also, it can be shown that a source distribution representation can only be used to represent the flow for a non-lifting body; that is, for lifting flow dipole or vortex distributions must be used.

As this stage, let's consider the solution of the flow about a non-lifting body of arbitrary geometry fixed in a uniform stream. Note that since G→0 on S∞ Φ already satisfy the condition S∞. The remaining condition, i.e. the condition is a stream surface is used to determine the source distribution strength.

Consider a source distribution method for representing non-lifting flow around a body of arbitrary geometry.

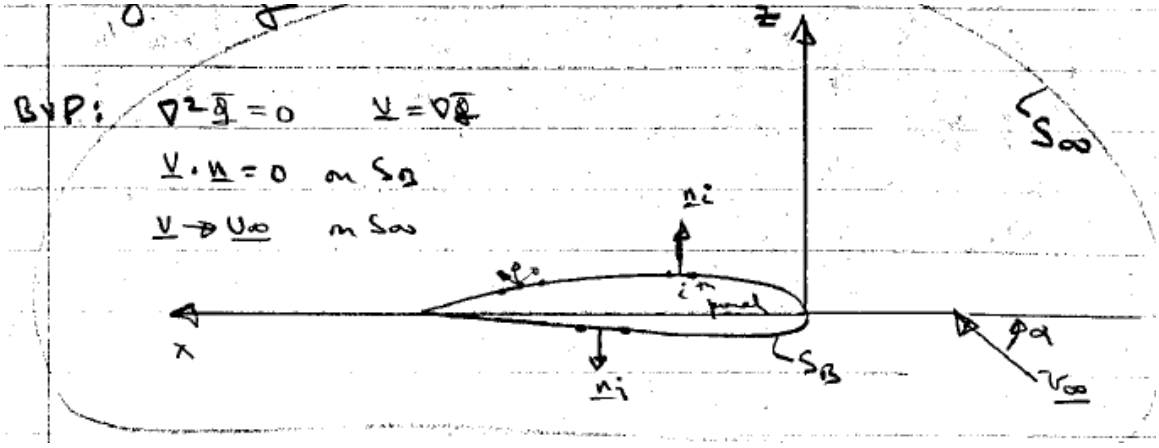

$\underline{V} = \underline{U}_\infty + \nabla\phi$: total velocity

U_∞ : uniform stream, $\nabla\phi$: perturbation potential due to presence of body

$\underline{U}_\infty = U_\infty(\cos\alpha\hat{i} + \sin\alpha\hat{j})$: note that for non-lifting flow Γ must be zero (i.e. for a symmetric foil $\alpha = 0$ or for cambered filed $\alpha = \alpha_{oLift}$)

$$\phi = \int_{S_B} \frac{K}{2\pi} \ln r ds : \text{source distribution on body surface}$$

Now, K is determined from the body boundary condition.

$\underline{V}\cdot\underline{n}=0$ i.e. $\underline{U_\infty}\cdot\underline{n}+\nabla\phi\cdot\underline{n}=0$ or $\frac{\partial\phi}{\partial n}=-\underline{U_\infty}\cdot\underline{n}$

i.e. normal velocity induced by sources must cancel uniform stream→

$$\frac{\partial}{\partial n}\int_{S_B}\frac{K}{2\pi}\ln r ds=-\underline{U_\infty}\cdot\underline{n}$$

This singular integral equation for K is solved by descretizing the surface into a number of panels over which K is assumed constant, i.e. we write

$$\frac{\partial}{\partial n_i}\sum_{j=1}^{M=\text{no. of panels}}\frac{Kj}{2\pi}\int_{Si}\ln r_{ij}dS_i=-\underline{U_\infty}\cdot\underline{n_i}\text{ , i=1,M, j=1,M}$$

where $r_{ij}=\sqrt{(x_i-x_j)^2+(z_i-z_j)^2}$ =distance from i[th] panel control point to $\underline{r_j}=$position vector along j[th] panel.

Note that the integral equation is singular since

$$\frac{\partial}{\partial n_i}\ln r_{ij}=\frac{1}{r_{ij}}\frac{\partial r_{ij}}{\partial n_i}$$

at for $r_{ij}=0$ this integral blows up; that is, when i=j and we trying to determine the contribution of the panel to its own source strength. Special care must be taken. It can be shown that the limit does exist at the integral equation can be written

$$\frac{K_i}{2\pi}\frac{\partial}{\partial n_i}\int_{S_j\to S_i}\ln r_{ij}dS_i=\frac{K_i}{2}$$

$$\frac{K_i}{2}+\sum_{\substack{i=1\\ j\neq i}}^{M}\frac{K_j}{2\pi}\int_{S_i}\frac{1}{r_{ij}}\frac{\partial r_{ij}}{\partial n_{ij}}dS_j=-\underline{U_\infty}\cdot\underline{n_i}$$

where $\frac{1}{r_{ij}}\frac{\partial r_{ij}}{\partial n_i}=\frac{1}{r_{ij}}\nabla_i r_{ij}\cdot\underline{n_i}=\frac{1}{r_{ij}}\left[\frac{\partial r_{ij}}{\partial x_i}n_{xi}+\frac{\partial r_{ij}}{\partial z_i}n_{zi}\right]=\frac{1}{r_{ij}^{\,2}}\left[(x_i-x_j)n_{xi}+(z_i-z_j)n_{zi}\right]$

where $r_{ij}^2=(x_i-x_j)^2+(z_i-z_j)^2$

Consider the i[th] panel

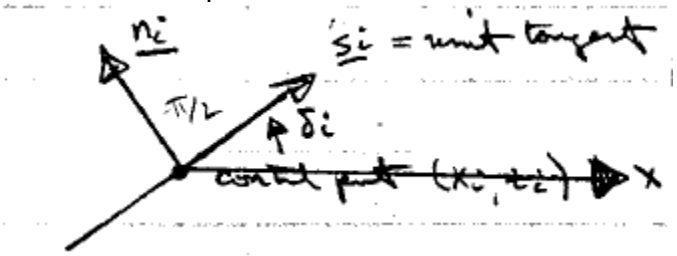

$$\underline{S_i} = \cos\delta_i \hat{i} + \sin\delta_i \hat{j}\ ,\ \underline{n_i} = \underline{S_i} \times \hat{j} = -\sin\delta_i \hat{i} + \cos\delta_i \hat{j}$$

$$n_{xi} = -\sin\delta_i\ , n_{zi} = \cos\delta_i$$

$$\frac{\partial}{\partial n}\int_{S_B} \frac{K}{2\pi} \ln r ds = -\underline{U_\infty} \cdot \underline{n}$$

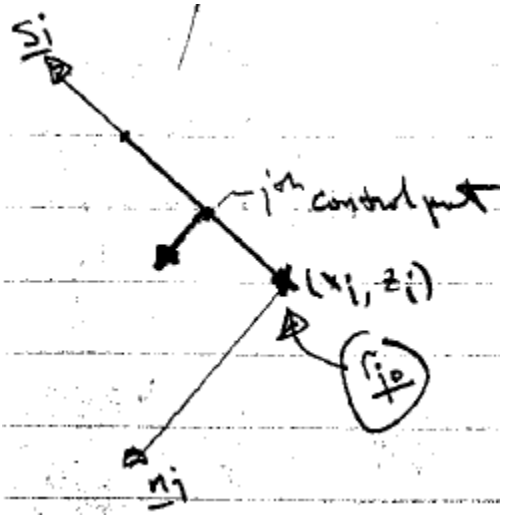

$\underline{r_j} = \underline{r_{j0}} + S\underline{S_i}$, $\underline{r_{j0}}$:origin of j[th] panel coordinate system, $S\underline{S_i}$: distance along j[th] panel

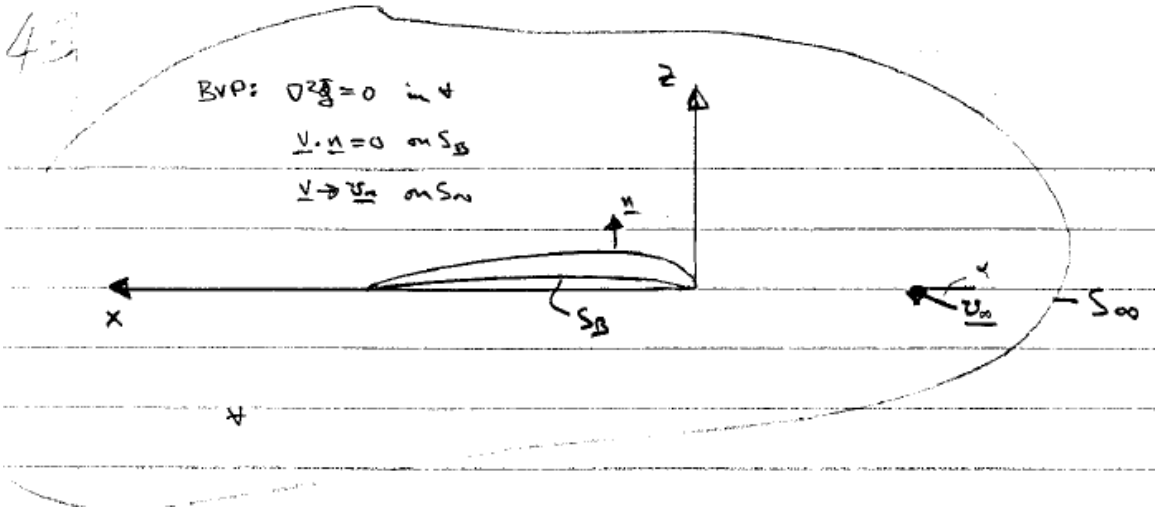

$$\underline{V} = U_\infty + \nabla\phi$$

$$\phi = \int_{S_B} \frac{K}{2\pi} \ln r ds$$

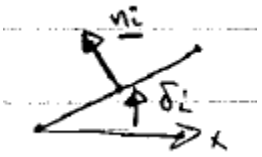

$$\underline{V}\cdot\underline{n} = 0 \rightarrow \frac{\partial}{\partial n}\int_{S_B}\frac{K}{2\pi}\ln r ds = -\underline{U_\infty}\cdot\underline{n}$$

$$\frac{K_i}{2} + \sum_{\substack{i=1\\ j\neq i}}^{M} \frac{K_j}{2\pi}\int_{S_i}\frac{1}{r_{ij}}\frac{\partial r_{ij}}{\partial n_{ij}} dS_j = -\underline{U_\infty}\cdot\underline{n_i} = -U_\infty \sin(\alpha - \delta_i),\ \underline{n_i} = -\sin\delta_i \hat{i} + \cos\delta_i \hat{j}$$

Let $\int_{S_i}\frac{1}{r_{ij}}\frac{\partial r_{ij}}{\partial n_{ij}} dS_j = I_j$ and $RHS_i = -U_\infty \sin(\alpha - \delta_i)$, then

$$\frac{K_i}{2} + \sum_{\substack{i=1\\ j\neq i}}^{M} \frac{K_j}{2\pi} I_j = RHS_i,\ I_j = \int_{S_j}\frac{(x_i - x_j)n_{xi} + (z_i - z_j)n_{zi}}{(x_i - x_j)^2 + (z_i - z_j)^2} dS_j$$

$$I_i = \int_0^{l_i} \frac{(x_i - x_{j0} - S_j n_{zj})n_{xi} + (z_i - z_{j0} - S_j n_{xj})n_{zi}}{(x_i - x_{j0} - S_j n_{zj})^2 + (z_i - z_{j0} - S_j n_{xj})^2} dS_j$$

$$= \int_0^{l_i} \frac{(x_i - x_{j0})n_{xi} + (z_i - z_{j0})n_{zi} + S_j(n_{xj}n_{zi} - n_{zj}n_{xi})}{(x_i - x_{j0})^2 + (z_i - z_{j0})^2 + 2S_j[-n_{zi}(x_i - x_{j0}) + n_{zj}(z_i - z_{j0})] + S_j^2} dS_j$$

$$= \int_0^{l_i} \frac{CS_j + D}{S_j^2 + 2AS_j + B} dS_j$$

where

$$A = -\cos\delta_j(x_i - x_{j0}) - \sin\delta_j(z_i - z_{j0})$$

$$B = (x_i - x_{j0})^2 + (z_i - z_{j0})^2$$

$$C = \sin(\delta_i - \delta_j)$$

$$D = -(x_i - x_{j0})\sin\delta_i + (z_i - z_{j0})\cos\delta_i$$

$$I_j = D\int_0^{l_i}\frac{1}{\mathrm{X}} dS_j + C\int_0^{l_i}\frac{S_i}{\mathrm{X}} dS_j = DI_{i1} + CI_{i2} \text{ where } \mathrm{X} = S_j^2 + 2AS_j + B$$

I_{j1} depends on if q<0 or >0 where $q = 4B - 4A^2$

$$I_{j2} = \frac{1}{2}\ln \mathrm{X} - AI_{i1}$$

$$\frac{K_i}{2} + \sum_{\substack{i=1\\ j\neq i}}^{M} \frac{K_j}{2\pi}\int_{S_j}\frac{(x_i - x_j)n_{xi} + (z_i - z_j)n_{zi}}{(x_i - x_j)^2 + (z_i - z_j)^2} dS_j = -\underline{U_\infty}\cdot\underline{n_i} = RHS_i$$

$$RHS_i = -U_\infty[-\cos\alpha\sin\delta_i + \sin\alpha\cos\delta_i] = -U_\infty\sin(\alpha - \delta_i)$$

$\frac{K_i}{2} + \sum_{\substack{i=1 \\ j\neq i}}^{M} \frac{K_j}{2\pi} I_i = RHS_i$: Matrix equation for K_i and can be solved using Standard methods such as Gauss-Siedel Iteration.

In order to evaluate Ij, we make the substitution

$x_j = x_{j0} + S_j S_{xj}$

$z_j = z_{j0} + S_j S_{xj} \rightarrow \underline{r_j} = \underline{r_{j0}} + S_j S_j$

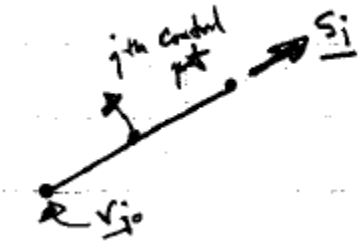

where Sj= distance along the j[th] panel $0 \le S_j \le l_i$

$S_{xj} = n_{zi} = \cos\delta_j$

$S_{zj} = n_{xi} = \sin\delta_j$

After substitution, Ij becomes

$$B - A^2 = (x_i - x_{j0})^2 + (z_i - z_{j0})^2$$
$$-\left[\cos^2\delta_j (x_i - x_{j0})^2 + \sin^2\delta_j (z_i - z_{j0})^2 + 2\cos\delta_j \sin\delta_j (x_i - x_{j0})(z_i - z_{j0})\right]$$
$$= (x_i - x_{j0})^2 (1 - \cos^2\delta_j) + (z_i - z_{j0})^2 (1 - \sin^2\delta_j) - 2$$

$$q = 4(B - A^2) = 4\left[(x_i - x_{j0})\sin\delta_i - (z_i - z_{j0})\cos\delta_i\right]^2$$

i.e. q>0 and as a result,

$$I_{j1} = \frac{2}{\sqrt{q}} \tan^{-1} \frac{2S_i + 2A}{\sqrt{q}} = \frac{1}{E} \tan^{-1} \frac{S_i + A}{E} \quad \text{where } \sqrt{q} = 2\sqrt{B - A^2} = 2E$$

$$I_j = DI_{j1} + C\left[\frac{1}{2}\ln \mathrm{X} - AI_{j1}\right] = (D - CA)I_{j1} + \frac{C}{2}\ln \mathrm{X}\Big|_0^{l_i}$$

$$= \frac{(D - CA)}{E}\left\{\tan^{-1}\frac{l_i + A}{E} - \tan^{-1}\frac{A}{E}\right\} + \frac{C}{2}\ln\left\{\frac{l_j z + 2Al_j + B}{B}\right\}$$

where $\mathrm{X} = S_i^2 + 2AS_j + B$

Therefore, we can write the integral equation in the form

$$\frac{K_i}{2} + \sum_{\substack{i=1 \\ j\neq i}}^{M} \frac{K_j}{2\pi} I_j = -U_\infty \sin(\alpha - \delta_i)$$

$$\begin{bmatrix} \frac{1}{2} & & \frac{k_j}{2\pi} I_j \\ & \ddots & \\ \frac{k_j}{2\pi} I_j & & \frac{1}{2} \end{bmatrix} \begin{bmatrix} K_i \end{bmatrix} = \begin{bmatrix} RHS_i \end{bmatrix}$$

which can be solved by standard techniques for linear systems of equations with Gauss-Siedel Iteration.

Once Ki is known,

$\underline{V} = U_\infty + \nabla\phi$

And p is obtained from Bernoulli equation, i.e.

$p = 1 - \frac{\underline{V} \cdot \underline{V}}{U_\infty^2}$

Mentioned potential flow solution only depend on is independent of flow condition, i.e. U∞, i.e. only is scaled

On the surface of the body Vn=0 so that

$C_p = 1 - \frac{V_S^2}{U_\infty^2}$ where $V_S = \underline{V} \cdot \underline{S}$ =tangential surface velocity

$V_S = \nabla\Phi \cdot \underline{S} = \underline{U_\infty} \cdot \underline{S} + \nabla\varphi \cdot \underline{S}$

$V_{S_i} = \underline{U_\infty} \cdot \underline{S_i} + \frac{\partial\varphi}{\partial S} = U_\infty \cos(\alpha - \delta_i) + Q_S$

where $\underline{U_\infty} \cdot \underline{S_i} = U_\infty \left(\cos\alpha\hat{i} + \sin\alpha\hat{j}\right) \cdot \left(\cos\delta_i\hat{i} + \sin\delta_i\hat{j}\right)$

$\phi_S = \frac{\partial\phi}{\partial S} = \frac{\partial}{\partial S} \int_{S_B} \frac{K}{2\pi} \ln r ds$

$\phi_{S_i} = \sum_{\substack{j=1 \\ j\neq i}}^{M} \frac{K_j}{2\pi} \int_{l_j} \frac{\partial}{\partial S_i} \left(\ln r_{ji}\right) dS_j$: j=i term is zero since source panel induces no tangential flow on itself. ($\int_{l_j} \frac{\partial}{\partial S_i} \left(\ln r_{ji}\right) dS_j = J_j$)

$\frac{\partial}{\partial S_i} \left(\ln r_{ij}\right) = \frac{1}{r_{ij}} \frac{\partial r_{ij}}{\partial S} = \frac{1}{r_{ij}} \nabla_i r_{ij} \cdot \underline{S_i}$

$= \frac{1}{r_{ij}} \left[\frac{\partial r_{ij}}{\partial x_i} S_{x_i} + \frac{\partial r_{ij}}{\partial z_i} S_{z_i}\right] = \frac{1}{r_{ij}^2} \left\{\left(x_i - x_j\right) S_{x_i} + \left(z_i - z_j\right) S_{z_i}\right\}$

where $S_{x_i} = \cos\delta_i, S_{z_i} = \sin\delta_i$

$$C_{p_i} = 1 - \left(\frac{V_{S_i}}{U_\infty} \right)^2 , V = -U_\infty \cos(\alpha - \delta_i) + \sum_{\substack{j=1 \\ i \neq j}} \frac{K_i}{2\pi} J_j$$

$$J_{ij} = \int_{l_i} \frac{1}{r_{ij}} \frac{\partial r_{ij}}{\partial S} dS_j = \int_{S_j} \frac{(x_i - x_j) n_{xi} + (z_i - z_j) n_{zi}}{(x_i - x_j)^2 + (z_i - z_j)^2} dS_j$$

$$= \int_0^{l_i} \frac{(x_i - x_{j0} - S_j S_{xj}) S_{xi} + (z_i - z_{j0} - S_j S_{zxj}) S_{zi}}{(x_i - x_{j0} - S_j S_{xj})^2 + (z_i - z_{j0} - S_j S_{zj})^2} dS_j$$

where $S_{x_i} = \cos\delta_i, S_{z_i} = \sin\delta_i,\ (x_i - x_{j0} - S_j S_{xj})^2 + (z_i - z_{j0} - S_j S_{zj})^2 = S_j^2 + 2AS_j + B$

$$(x_i - x_j)\cos\delta_i + (z_i - z_{i0})\sin\delta_i + S_j(-S_{xj} S_{xi} - S_{zj} S_{zi}) - \cos\delta_j \cos\delta_i - \sin\delta_j \sin\delta_i$$

$$= \int_0^{\lambda_i} \frac{CS_j + D}{S_j^2 - AS_j - C} dS_i$$

$$D = (x_i - x_{j0})\cos\delta_i + (z_i - z_{j0})\sin\delta_i$$

$$C = -\cos(\delta_i - \delta_j) = DI_{j1} + CI_{j2} = DI_{j1} + C\left\{ \frac{1}{2} \ln \mathrm{X} - AI_{j1} \right\}$$

$$J_j = (D - AC) I_{j1} + \frac{C}{2} \ln \mathrm{X} = \frac{D - AC}{E} \left\{ \tan^{-1} \frac{l_j + A}{E} - \tan^{-1} \frac{A}{E} \right\} + \frac{C}{2} \ln \frac{l_j^2 + 2Al_j + B}{B}$$

$$D - AC = (x_i - x_{j0})\cos\delta_i + (z_i - z_{j0})\sin\delta_i$$

$$-\left[-(x_i - x_{j0})\cos\delta_i - (z_i - z_{j0})\sin\delta_i \right](-\cos(\delta_j - \delta_i))$$

$$\left[(x_i - x_{j0})\cos\delta_i + (z_i - z_{j0})\sin\delta_i \right](-\sin\delta_i \sin\delta_j - \cos\delta_i \cos\delta_j)$$

$$= (x_i - x_{j0})\left[\cos\delta_i - \sin\delta_i \sin\delta_j \cos\delta_j - \cos\delta_i \cos^2\delta_i \right]$$

$$(z_i - z_{j0})\left[\sin\delta_i - \sin\delta_i \sin^2\delta_j - \cos\delta_i \cos\delta_j \sin\delta_j \right]$$

$$= (x_i - x_{j0})\left[\cos\delta_i (1 - \cos^2\delta_j) - \sin\delta_i \sin\delta_j \cos\delta_j \right]$$

$$(z_i - z_{j0})\left[\sin\delta_i (1 - \sin^2\delta_j) - \cos\delta_i \cos\delta_j \sin\delta_j \right]$$

$$= (x_i - x_{j0})\sin\delta_j \left[\cos\delta_i \sin\delta_j - \sin\delta_i \cos\delta_j \right] - (z_i - z_{j0})\cos\delta_j \left[-\sin\delta_i \cos\delta_j + \cos\delta_i \sin\delta_j \right]$$

where $\frac{D - AC}{E} = -\sin(\delta_i - \delta_j)$

53

A Class of Airfoils Designed for High Lift in Incompressible Flow

Robert H. Liebeck*
Douglas Aircraft Company, McDonnell Douglas Corporation, Long Beach, Calif.

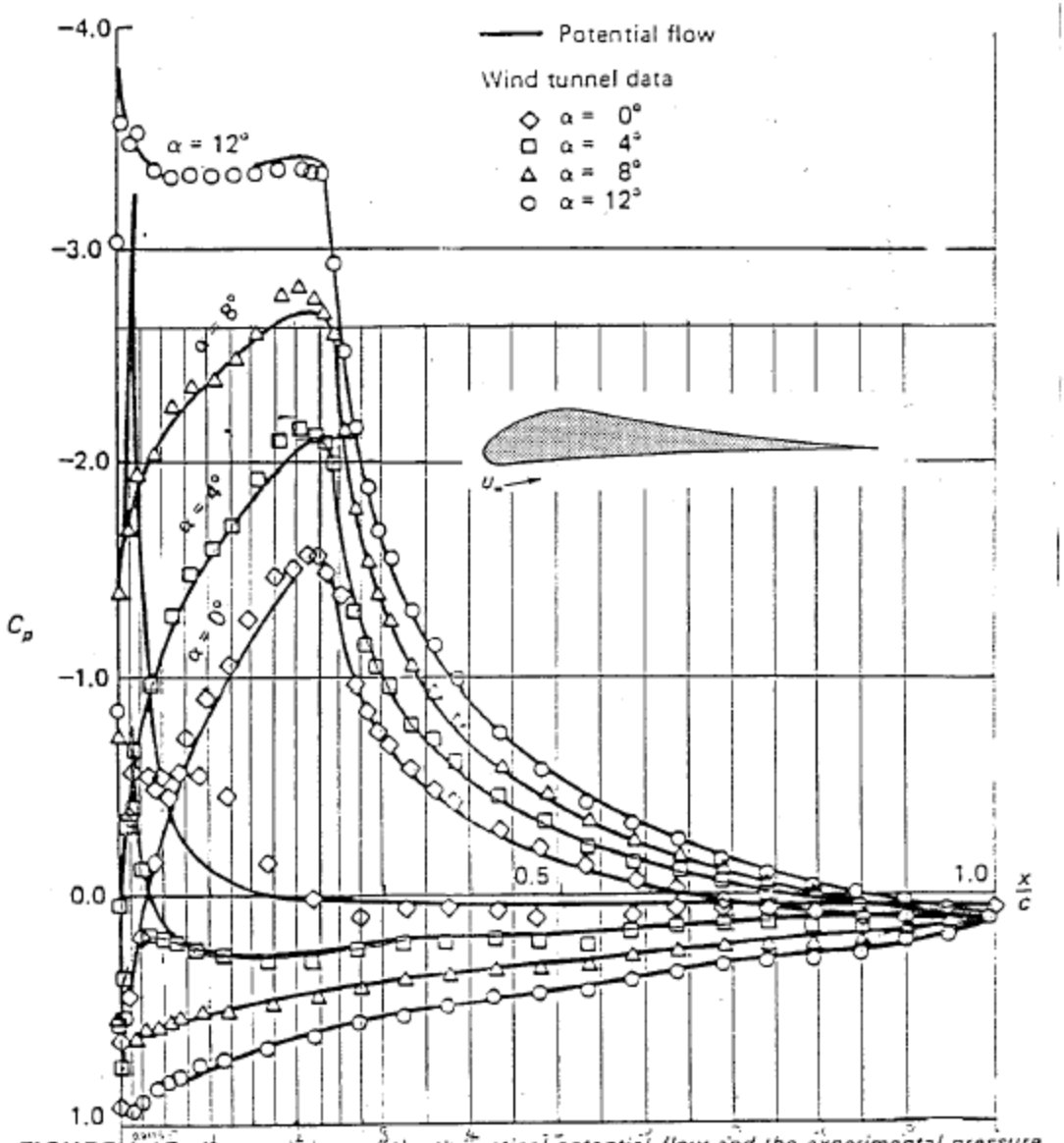

FIGURE 4-15 *A comparison of the theoretical potential-flow and the experimental pressure distribution for a high-lift, single-element airfoil, $Re_c = 3 \times 10^6$ (from Ref. 4.6).*

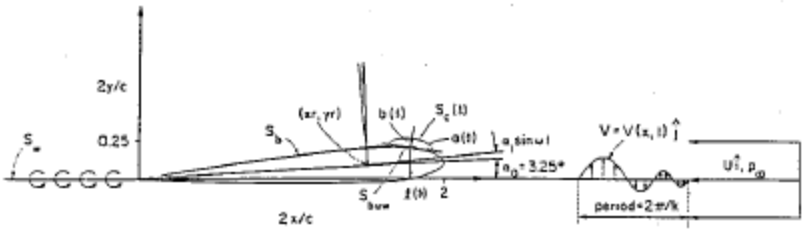

Figure 1. Cavity and foil geometry.

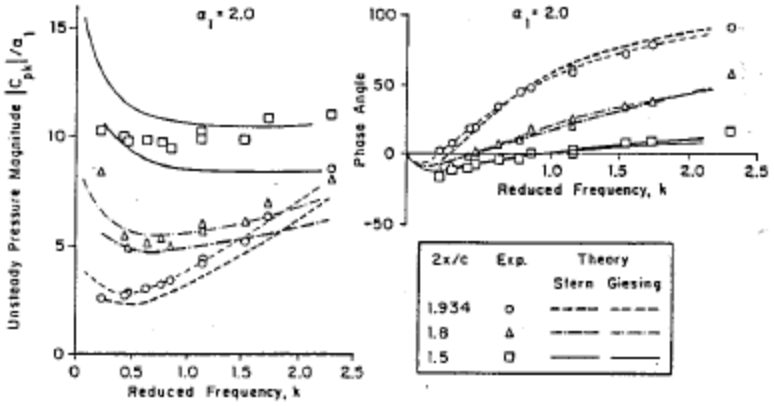

Figure 2. Noncavitating flow unsteady pressure magnitude and phase angle.

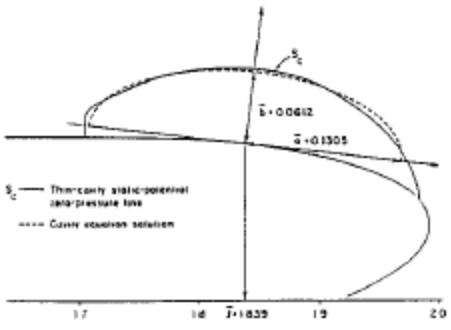

Figure 3. Steady-cavity solution: $\alpha_0 = 4.3°$.

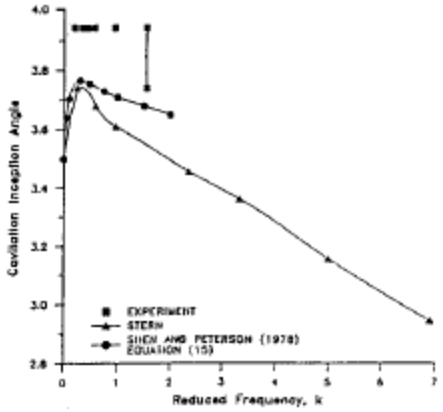

Figure 4. Cavitation inception angles: $\alpha_1 = .95°$.

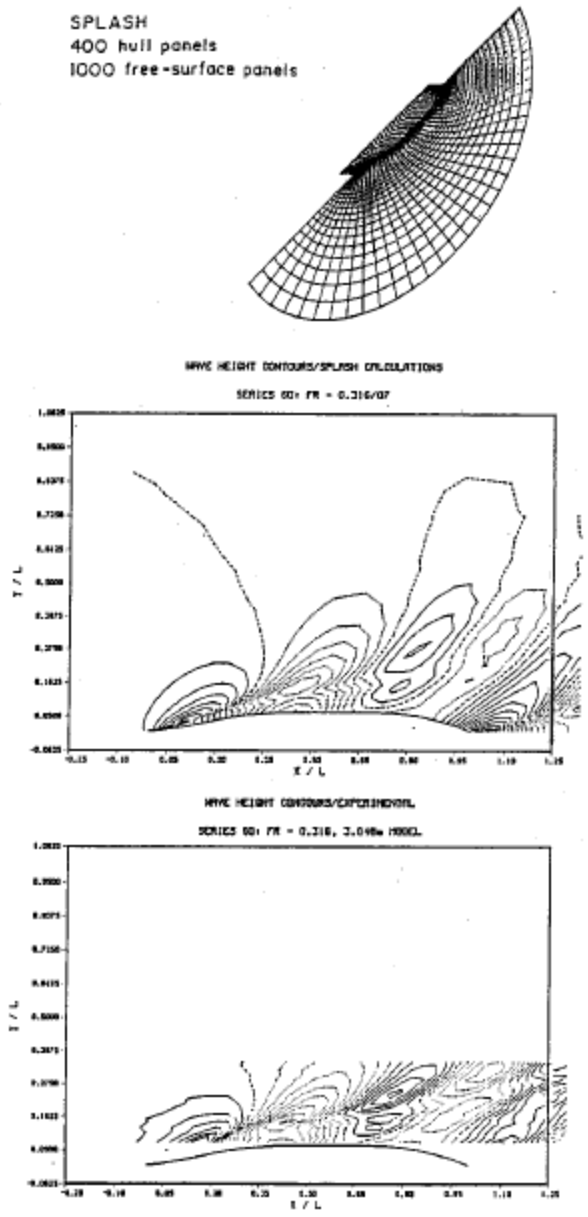

Figure 10. SPLASH hull and free-surface panels and SPLASH and experimental wave-height contours.

56

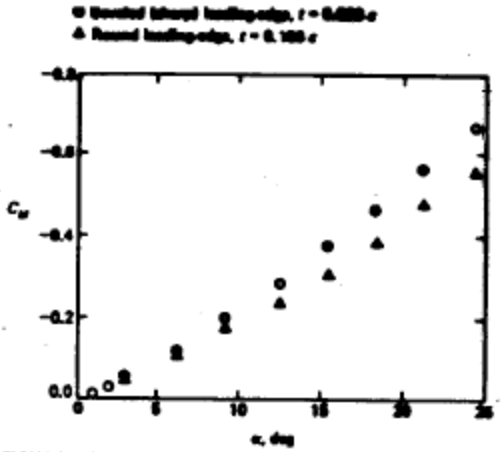

FIGURE 6-38 *The moment coefficient (about the apex) for thin, flat delta wings for which AR = 1.5, $Re_c = 6 \times 10^4$ (data from Ref. 6.19).*

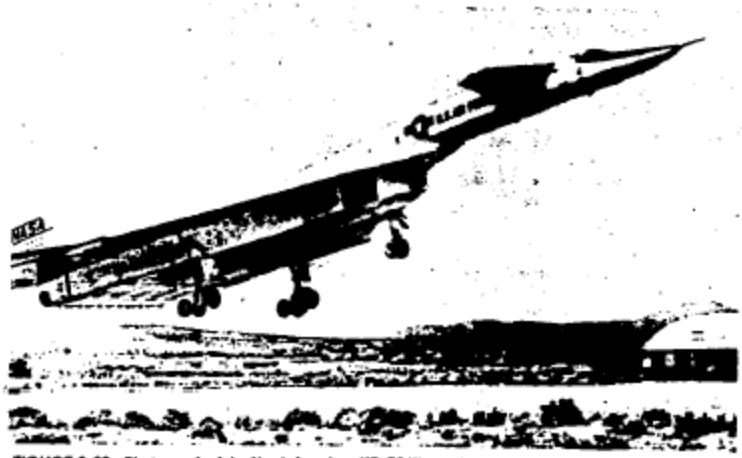

FIGURE 6-39 *Photograph of the North American XB-70 illustrating the use of canards (Courtesy, NASA).*

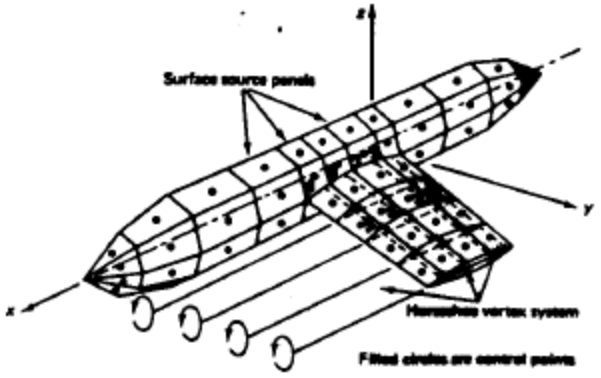

FIGURE 6-40 *Source and vortex lattice panel arrangement for a wing/body configuration for zero yaw, i.e., xz plane is a plane of symmetry.*

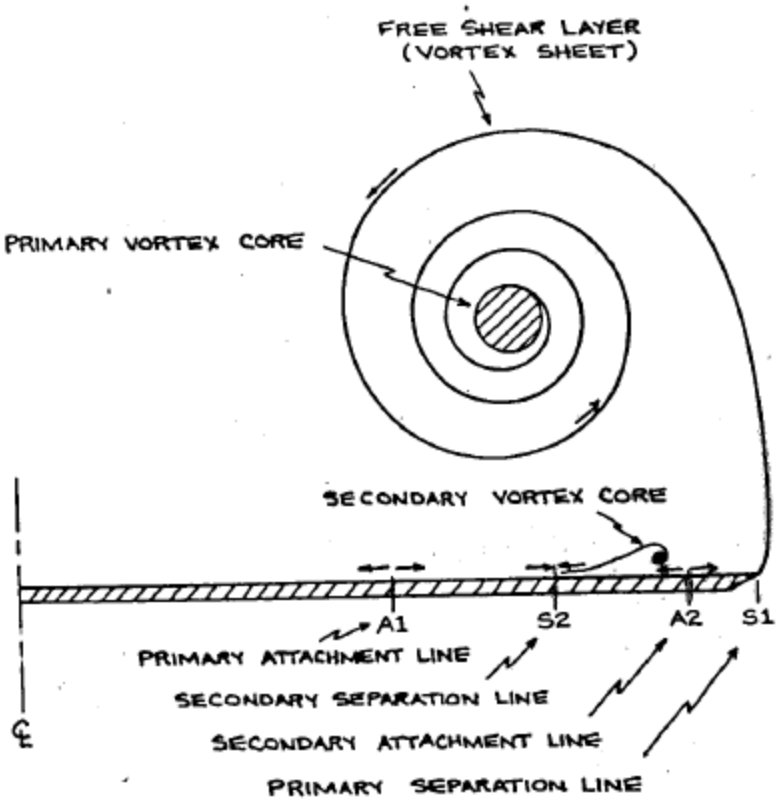

Figure 4.1.6 - Flow pattern in crossflow plane on delta wing

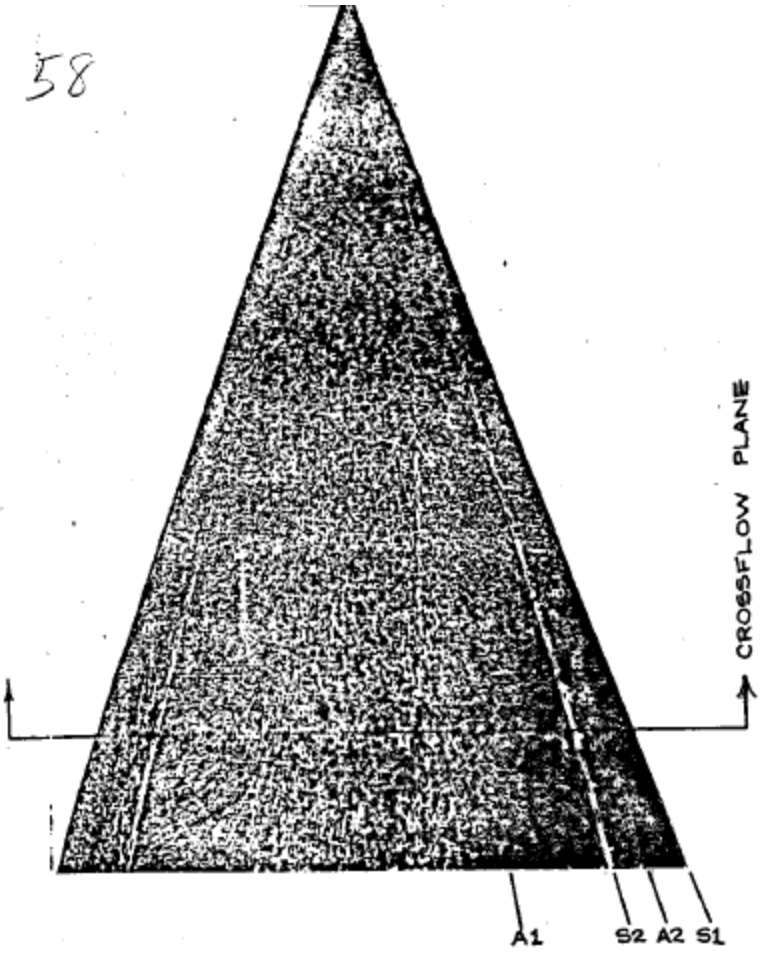

(From Marsden, Simpson, and Rainbird, 1958)

Figure 4.1.5 - Surface flow visualization on upper surface of delta wing (α = 14°)

59

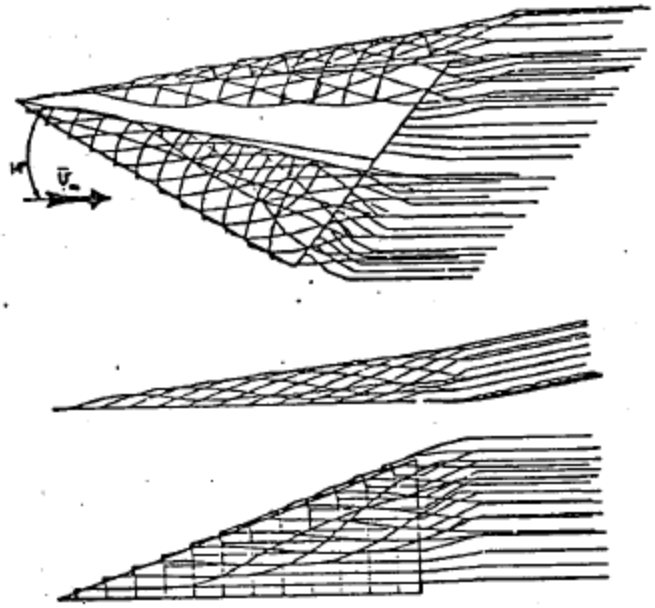

(From Kandil, Mook, & Nayfeh, 1976)

Figure 5.2.2 - Typical solution of wake shape for a delta wing using Kandil, Mook, & Nayfeh model

60

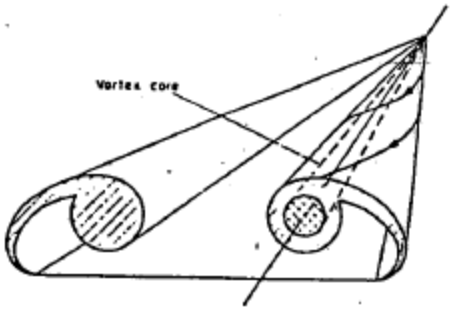

(From Hall, 1966)

Figure 4.1.3 - Vortex cores over slender delta wing

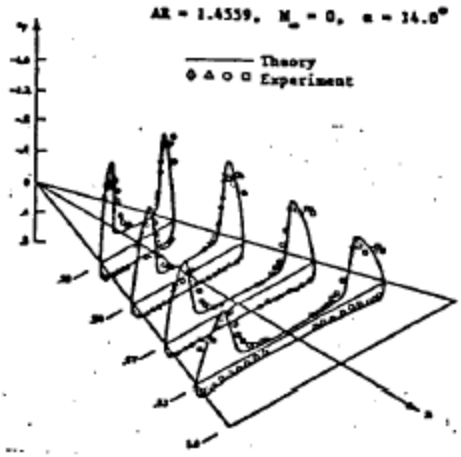

(From Smith, 1978)

Figure 4.1.4 - Pressure distribution on upper surface of delta wing

61

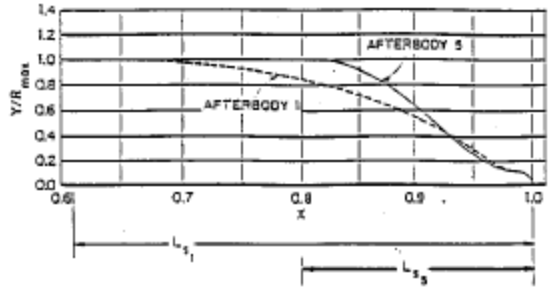

Figure 21. Geometric Data for DTMSRDC Afterbodies 1 and 5

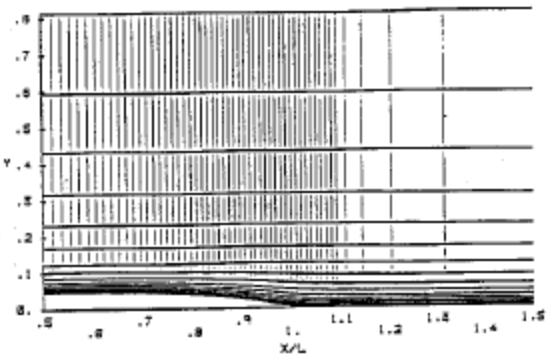

Figure 22. Large-Domain Grid for Afterbody 1

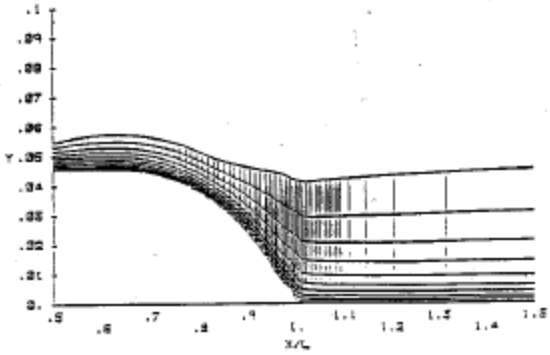

Figure 23. Small-Domain Grid for Afterbody 1

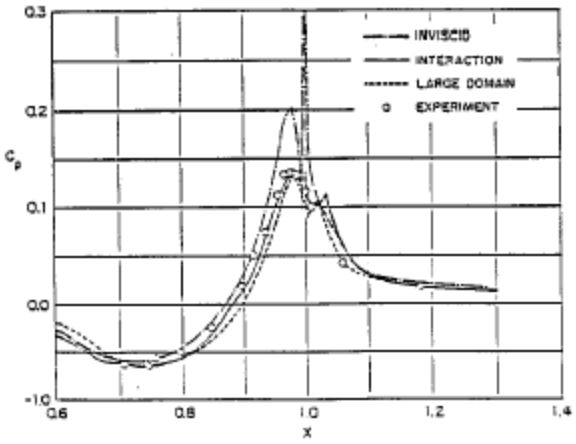

Figure 24. Pressure Distribution on the Surface of the Body and Along the Wake Centerline